0022-3530/93 $3.00

# Leucogranites from the Eastern Part of the South Mountain Batholith, Nova Scotia

*by* D. BARRIE CLARKE[1], MICHAEL A. MACDONALD[2], PETER H. REYNOLDS[1], AND FRED J. LONGSTAFFE[3]

[1]*Department of Earth Sciences, Dalhousie University, Halifax, Nova Scotia, Canada B3H 3J5*
[2]*Nova Scotia Department of Natural Resources, Halifax, Nova Scotia, Canada B3J 2T9*
[3]*Department of Geology, University of Western Ontario, London, Ontario, Canada N6A 5B7*

(*Received 20 May 1991; revised typescript accepted 28 September 1992*)

## ABSTRACT

The South Mountain Batholith is a peraluminous granitic complex ranging in composition from biotite granodiorite to muscovite–topaz 'leucogranite'. Leucogranitic rocks (with generally $<2\%$ biotite) form a minor part ($\sim 1{\cdot}5\%$) of the batholith, and are of two types: (1) 'associated leucogranites' occurring as relatively small zones in fine-grained leucomonzogranites; and (2) 'independent leucogranites' forming generally larger bodies having no particular spatial association with other rock types. Mean chemical compositions of these two types of leucogranite are as follows (associated, independent): $Na_2O$ (3·46, 3·83), $K_2O$ (4·40, 4·09), and $P_2O_5$ (0·26, 0·45) in wt.%; Li (149, 281), F (1199, 2712), Rb (393, 725), U (7·4, 4·4), Nb (12·8, 23·4), Ta (2·9, 7·1), and Zr (52, 31) in ppm. Rare earth elements also differ between the two types (associated, independent): ΣREE (34·1 ppm, 19·9 ppm); and in the degree and variability of heavy REE fractionation ($Gd_N/Yb_N = 4{\cdot}6 \pm 2{\cdot}2$, $2{\cdot}0 \pm 0{\cdot}7$). In addition, associated leucogranite has REE compositions similar to those of its host rocks. Mean $\delta^{18}O$ values (associated $+11{\cdot}2 \pm 1{\cdot}2‰$, independent $+11{\cdot}4 \pm 0{\cdot}5‰$; relative to SMOW) are comparable with the mean for the entire South Mountain Batholith ($+10{\cdot}8 \pm 0{\cdot}7‰$). Radiometric dating ($^{40}Ar/^{39}Ar$ on muscovite) shows that both types of leucogranite have identical ages of $372 \pm 3$ Ma, equivalent to ages determined by other techniques for granodiorite and monzogranite samples elsewhere in the batholith. Field relations and geochemistry suggest that the associated leucogranite results from an open-system interaction between a fluid and its host leucomonzogranite, whereas the independent leucogranite bodies are discrete intrusions of highly fractionated melts that underwent closed-system, late-magmatic to post-magmatic fluid alteration. Where mineralized, the associated leucogranite characteristically hosts greisen-type or disseminated polymetallic mineralization, whereas the independent leucogranite hosts pegmatitic or disseminated polymetallic mineralization.

## INTRODUCTION

Leucogranitic rocks typically occur either as relatively small individual bodies or, as in the South Mountain Batholith, as minor and late components of large peraluminous batholithic complexes in continent–continent collisional zones. Genetically, these leucogranitic rocks can be the products of: (1) minimum partial melting of metasedimentary rocks (Strong & Hanmer, 1981); (2) extensive fractional crystallization of tonalitic–granodioritic–monzogranitic parental magmas (Monier *et al.*, 1984); (3) late magmatic and post-magmatic hydrothermal alteration (Monier *et al.*, 1984); (4) granitization (Searle & Fryer, 1986); or (5)

 

some combination of these origins. Peraluminous leucogranitic rocks are commonly associated with Sn–W–U–Mo mineralization (e.g., Tischendorf, 1977; Groves & McCarthy, 1978; Evans, 1982; Strong, 1988), including those of the South Mountain Batholith. There is a former tin mine in the extreme western part of the batholith (Kontak, 1990), and a variety of smaller mineral deposits occur throughout the batholith (O'Reilly *et al.*, 1982; Chatterjee & Clarke, 1985), all associated with leucogranitic rocks. In most cases, however, any genetic connections between leucogranitic bodies and their mineral deposits are inferred from spatial relationships, as opposed to being demonstrated directly through some combination of geochemistry and geochronology.

In the South Mountain Batholith of southern Nova Scotia, we recognize two principal kinds of leucogranitic occurrences:

(1) associated leucogranitic bodies that are characteristically affiliated with fine-grained leucomonzogranitic rocks; and

(2) independent leucogranitic bodies that show no systematic spatial relationship with other rock types. As used here, 'independent' has no temporal or genetic connotations.

At one locality (Walsh Brook; Fig. 1) several small leucogranite bodies have uncertain affinities, and we designate them as 'unclassified leucogranite'.

In this paper we examine the field relations, mineralogy, textures, chemical compositions, and ages of these leucogranite occurrences with a view to discriminating between the associated and independent leucogranitic rocks, and to determining their origins and economic potential.

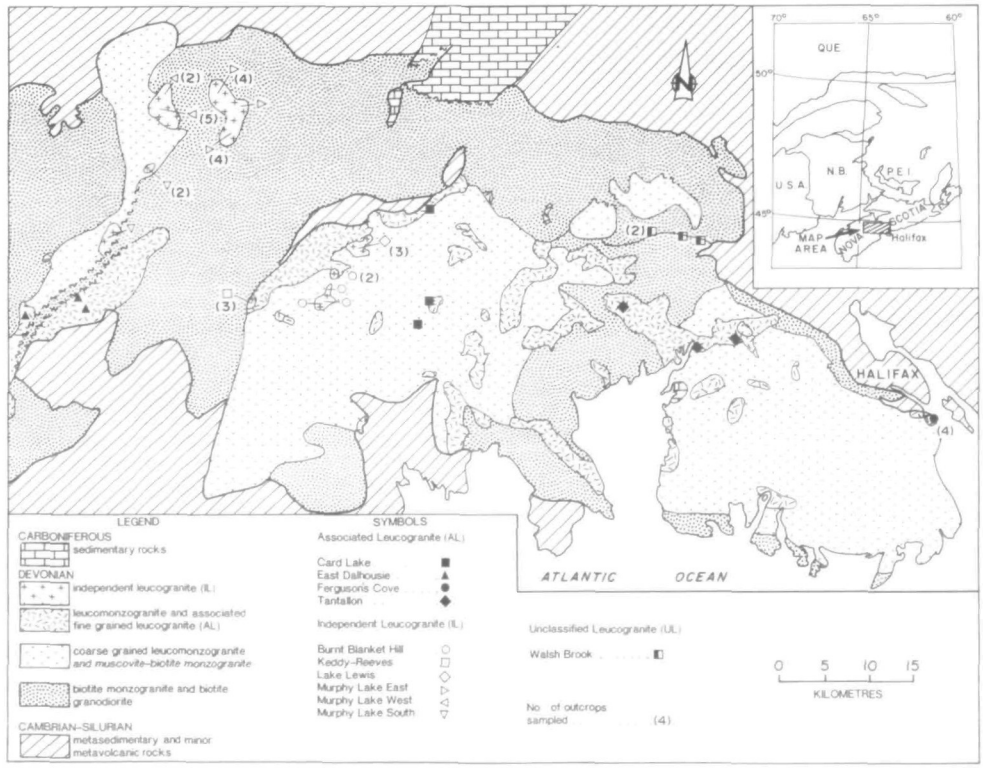


FIG. 1. Simplified geological map of the eastern part of the South Mountain Batholith, showing sites sampled for the present study.

## NOMENCLATURE

Previous terms used for leucogranitic rocks in the South Mountain Batholith include alaskite (McKenzie, 1974; Smith, 1974), leucoadamellite (McKenzie, 1974; Charest, 1976), leucomonzogranite (O'Reilly *et al.*, 1982; Clarke & Muecke, 1985), and leucogranite (Chatterjee & Muecke, 1982; MacDonald *et al.*, 1992). We use the Streckeisen (1976) definition whereby 'leuco' refers to 0–6% ferromagnesian minerals, and 'leucogranitic rocks' as a general name for leucocratic monzogranites, syenogranites, and alkali feldspar granites. Most of our leucogranitic rocks contain $<2\%$ dark minerals, so they are at the extreme light-coloured end of the leucocratic range. In the South Mountain Batholith, biotite is the dominant ferromagnesian mineral, but magmatic cordierite and garnet also occur, and chlorite is a common alteration product of all three. Oxide minerals are rare.

## GENERAL FEATURES OF THE SOUTH MOUNTAIN BATHOLITH

### *Setting and age*

The South Mountain Batholith underlies $\sim 7300\ km^2$ of southwestern Nova Scotia. It intrudes predominantly flyschoid metawackes and metapelites of the Cambro-Ordovician Meguma Group (Taylor, 1969). Along its northwestern margin it intrudes a conformable succession of metavolcanic and metasedimentary rocks that range in age from Ordovician (White Rock Formation) to Lower Devonian (Torbrook Formation) (Taylor, 1969; Smitheringale, 1973). The Acadian orogeny deformed and regionally metamorphosed these rocks to greenschist–amphibolite grade at 390–405 Ma (Reynolds *et al.*, 1981); Keppie & Dallmeyer (1987) extend this event to 375 Ma. The eastern part of the batholith lies entirely within greenschist facies host rocks.

Clarke & Halliday (1980) obtained three whole-rock Rb–Sr isochron ages for different facies of the batholith: $371{\cdot}8 \pm 2{\cdot}2$ Ma for the early biotite granodiorite; $364{\cdot}3 \pm 1{\cdot}3$ for a later monzogranite; and $361{\cdot}2 \pm 1{\cdot}4$ Ma for a suite of late porphyries and aplites. Harper (1988) reproduced the Rb–Sr apparent age of the monzogranite, but indicated a primary crystallization age of $371 \pm 5$ Ma for the muscovite. He also obtained an age of $361 \pm 2$ Ma for the leucomonzogranite, but estimated a primary crystallization age of $369{\cdot}6 \pm 1$ Ma for muscovite. Harper also determined U–Pb monazite ages of $374{\cdot}3 \pm 1{\cdot}9$ Ma for the monzogranite and $372{\cdot}8 \pm 2{\cdot}1$ Ma for the leucomonzogranite. Richardson *et al.* (1989) used Rb–Sr data from the western part of the batholith to propose mid-Carboniferous magmatism for the Meguma Zone; however, Kontak & Cormier (1991) concluded that 'young' ages in this area are the result of several tectono-thermal resetting events. Thus, in general, no measurable age differences exist between all major magmatic rock types in the eastern part of the batholith.

Coarse subaerial clastic sediments and marine carbonates of the Horton and Windsor Groups of Lower Carboniferous age unconformably overlie the batholith; thus, its emplacement, crystallization, uplift, and erosion all occurred in a narrow time interval between post-Emsian and early Tournaisian.

### *Internal structure and composition*

The South Mountain Batholith truncates regional Acadian structures and is, for the most part, massive and undeformed. Pervasive NE-trending primary flow features, and orthogonal vein, shear, and joint orientations, developed throughout the batholith, suggest that emplacement and crystallization occurred during the waning stages of Acadian

deformation (Horne *et al.*, 1988). MacDonald *et al.* (1992) conducted detailed geological mapping of the batholith, and divided it into six main rock types ranging from biotite granodiorite (the least evolved) to muscovite–topaz 'leucogranite' (leucocratic alkali feldspar granite—the most evolved). They assigned these rocks to 13 plutons that can be grouped as early (mostly granodiorite and monzogranite) and late (mostly leucomonzogranite and leucogranite).

The general mineral assemblage of unaltered rocks in the batholith is quartz + alkali feldspar + plagioclase + muscovite ± biotite ± cordierite ± garnet ± andalusite ± topaz ± ilmenite. Magnetite is rare to absent. Typical bulk chemical compositions have 65–75% $SiO_2$, 0·4–2·0% CaO, and molar values of $Al_2O_3/(CaO+Na_2O+K_2O)$ (i.e., A/CNK) between 1·1 and 1·3. The rocks, therefore, satisfy many of the characteristics of the so-called ilmenite-series, or S-type granites (Clarke & Muecke, 1985), although we prefer the non-genetic term 'peraluminous'.

Fractional crystallization of plagioclase, biotite (with included accessories such as zircon, apatite, and monazite), and alkali feldspar controls much of the chemical variation in the plutons (McKenzie & Clarke, 1975; Smith *et al.*, 1986; Clarke & Chatterjee, 1988). In the later leucomonzogranitic and leucogranitic rocks, fluid–melt and fluid–rock interaction may control the compositional variation (Kontak *et al.*, 1988; MacDonald & Clarke, 1991).

Several workers have presented isotopic data bearing on the origin of the batholith, including $^{18}O$ data (Longstaffe *et al.*, 1980; Kontak *et al.*, 1988), Rb–Sr data (Clarke & Halliday, 1980; O'Reilly *et al.*, 1985; Richardson *et al.*, 1989; Kontak & Cormier, 1991), and Nd–Sm data (Clarke *et al.*, 1988). These studies indicate that the batholith and other Meguma Zone granites developed by anatexis of a predominantly sedimentary, or a mixed sedimentary–altered volcanic source different from the Meguma Group. Recent isotopic work on lower crustal xenoliths, from a lamprophyric dyke in the eastern part of the Meguma Zone, shows that they have Sr, Nd, and Pb compositions suitable to be a source for the peraluminous granitoid rocks of the Meguma Zone (Eberz *et al.*, 1991).

## THE LEUCOGRANITIC ROCKS

### *Field relations and petrography*

The independent leucogranitic rocks occur as discrete bodies in the central and western portions of the study area (Fig. 1); individual bodies range in area from a few tens of square metres to 5 $km^2$, and they account for ~0·7% of the batholith area. Their host rocks are granodiorite, monzogranite, and leucomonzogranite, and their contacts are invariably sharp and intrusive (Fig. 2a). In contrast, the associated leucogranitic bodies are always hosted by fine-grained leucomonzogranite; they occur as small zones (generally $< 100$ $m^2$) and are too small to show in Fig. 1. We estimate their areal extent to be $< 1\%$ of the batholith. Contacts with their hosts, where visible, are invariably gradational (Fig. 2b). Five small individual bodies of leucogranitic rock cropping out in the northeastern end of the batholith (the unclassified leucogranites from the Walsh Brook locality; Fig. 1) have sharp intrusive contacts suggestive of independent leucogranite.

Associated leucogranitic rocks are mostly fine to medium grained, with equigranular or porphyritic textures (Table 1; Fig. 2b), and they typically resemble the host leucomonzogranite in texture and grain size. In contrast, independent leucogranite rocks commonly range from fine to very coarse grained, and have aplitic, equigranular, porphyritic, seriate, and pegmatitic textures, all of which can occur within a single outcrop (Fig. 2a). The unclassified leucogranite bodies of Walsh Brook are fine to medium grained with equigranular texture, and they cannot be classified texturally as either associated or independent.

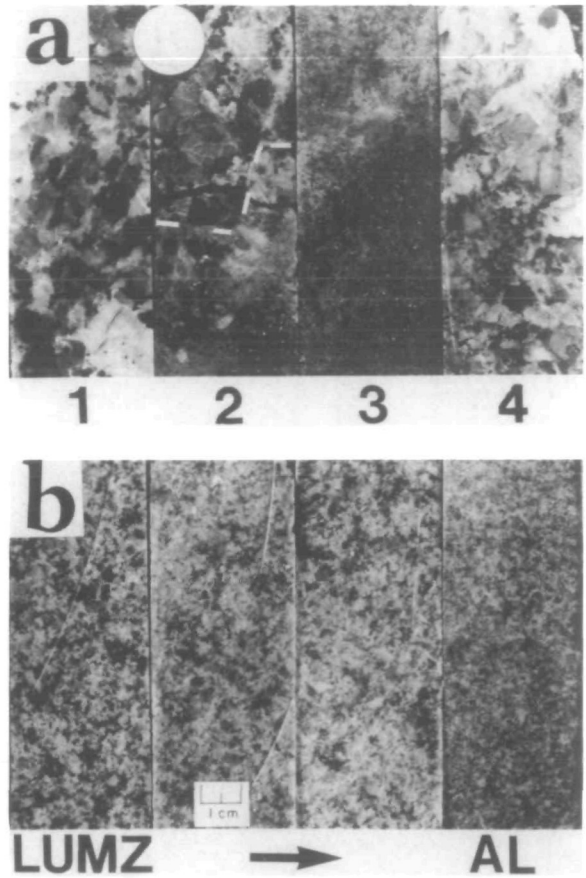


FIG. 2. Photographs of drill core, showing typical textures and contact relations for independent and associated leucogranite types. (a) 1, Biotite granodiorite; 2, sharp intrusive contact of Murphy Lake West independent leucogranite (below) with biotite granodiorite (above); 3, hematized and fresh equigranular independent leucogranite of Murphy Lake West; 4, medium- to coarse-grained and pegmatitic part of Murphy Lake West body. (b) Four split diamond drill cores from Long Lake (O'Reilly *et al.*, 1982), showing a gradational contact between a host leucomonzogranite (LUMZ) and an associated leucogranite (AL). This transition occurs over a distance of 1–2 m.

Petrographic investigation of 25 associated, 34 independent, and six unclassified leucogranite samples, point counting (1000 points) of 48 thin sections, and microprobe analysis of 14 polished thin sections have defined some differences between the two leucogranitic types (Table 1), as summarized below.

Characteristics of the associated type are: normal and reversely zoned plagioclase of compositions $An_{0-12}$ representing mostly primary magmatic compositions; modal percentages of muscovite ranging from 2·2 to 12·5% (Fig. 3), with averages of 6·8–7·5% for individual bodies [muscovite occurs predominantly as secondary anhedral replacement products of alkali feldspar, biotite, and plagioclase, although minor to common euhedral (primary?) crystals occur]; modal percentages of biotite ranging from 1·3 to 2·6%, with averages of 1·5–1·9% for individual bodies; chlorite as pseudomorphs after biotite; andalusite as trace amounts; and no topaz.

In contrast, typical petrographic features in independent types are: dominantly unzoned albitic plagioclase, with compositions generally in the range $An_{0-5}$ and probably

TABLE 1

*Comparative petrographic data for leucogranitic rocks from the eastern South Mountain Batholith*

| | *Texture* | | *Mineralogy* | | | | | | | | | | *Mineralization* | | | | | | *Ref* |
|---|---|---|---|---|---|---|---|---|---|---|---|---|---|---|---|---|---|---|---|
| | *Grain size* | *Textural types* | *Plagioclase* | | *K-feldspar* | | | *Muscovite (%)* | | | *Biotite (%)* | | | *Topaz* | *Andal.* | *Tour* | *Fluor* | *Type* | *Commodities* | |
| | | | *Comp An* | *Zoning* | *Host* | *Primary* | *Lamellae* | *Repl* | *Range* | *Av* | *Type* | *Range* | *Av.* | *Alt* | | | | | | | |
| | | | | | | | | | | *Associated leucogranitoids* | | | | | | | | | | | |
| Card Lake | F–M | PO+EQ⩾AP+PG+MA | 0–1 | U | | | | | | | | | | | 0 | | 0 | 0 | G | U,Sn,Cu,Mo,Pb,Zn | 1,2 |
| East Dalhousie | F–M | PO+EQ⩾MG | 0–11 | N,R>U | O,M | | R>P | x | 3·6–12·3 | 7·5 | A⩾E | 1·3–1·6 | 1·5 | F,C,M | 0 | 0–tr | 0 | 0 | D | U | 3,4 |
| Ferguson's Cove | F–M | PO⩾MG | 1–12 | R,N>U | O⩾M | | R,P | x | 5·5–9·8 | 6·9 | A⩾E | 1·6–2·2 | 1·9 | C>F,M | 0 | 0–tr | 0 | 0 | G | As,Cu | 5 |
| Tantallon | F–M | PO+EQ+AP+GR⩾PG+MG+SE+MA | 1–10 | N,R>U | O⩾M | | R | | 2·2–12·5 | 6·8 | A⩾E | 1·4–2·6 | 1·8 | C>M>F | 0 | 0–tr | 0 | 0 | G | As,Cu | 5 |
| | | | | | | | | | | *Independent leucogranitoids* | | | | | | | | | | | |
| Burnt Blanket Hill | F–M | PO+EQ>PG | 0–2 | U>R | O>M | | P | x | 7·2–19·8 | 12·3 | E>A | 0–2·0 | 0·6 | M>F,H | 0–tr | 0–0·6 | 0 | 0 | P | W,Cu | 1,2 |
| Keddy-Reeves | M | EQ | 0–2 | U | O | | | | 6·0–16·8 | 10·5 | E>A | tr.–0·1 | 0·1 | F | 0–0·7 | 0 | 0 | 0 | P | Sn,W,Li,Ta,U | 3 |
| Lake Lewis | F–M | EQ>PO⩾PG+AP | 0–6 | U | O⩾M | | R,P | x | 9·8–17·7 | 14·7 | E>A | tr–1·3 | 0·4 | M>F | 0–tr | 0–0·5 | 0 | tr | P | Mo | 2 |
| Murphy Lake East | F–VC | PO+EQ+PG⩾AP+MG+SE+GR+MA | 1–14 | N>U | O | | | x | 3·2–16·7 | 10·3 | E>A | 0–3·9 | 1·7 | H>M>F | 0 | 0 | 0 | 0 | D | U,F | 4 |
| Murphy Lake South | F–VC | PO+EQ>PG+AP | n.d. | U,N | O | | R,P | x | 2·5–10·5 | 5·8 | | 0·7–2·3 | 1·6 | H,M,F | 0 | 0 | 0 | 0–tr. | | | 4 |
| Murphy Lake West | F–VC | PO+EQ+PE⩾AP+MG+SE+GR+MA | 0–1 | U | O⩾M | | | x | 8·8–28·5 | 16·4 | | 0–1·4 | 0·3 | H>M>F | 0–tr. | 0 | 0 | 0 | D | U,F,P,Ba | 4 |
| | | | | | | | | | | *Unclassified leucogranitoids* | | | | | | | | | | | |
| Walsh Brook | F–M | EQ⩾GR | 2–14 | N>R>U | O | | P | x | 5·8–12·4 | 8·7 | A⩾E | 1·0–2·0 | 1·5 | C>F | 0 | 0–tr. | 0–0·1 | 0 | | | 6 |

*Texture*
Grain size: F—fine (<0·1 cm); M—medium (0·1–0·5 cm); C—coarse (0·5–3·0 cm); VC—very coarse (>3·0 cm)
Texture: AP—aplite; EQ—equigranular; GR—graphic; MA—mica aplite (coarse phenocrysts of muscovite ± biotite ± quartz) in aplitic matrix; MG—megacrystic, PG—pegmatitic, PO—porphyritic; SE—seriate.
*Mineralogy*
Plagioclase: Comp. An—anorthite content; Zoning—N, normal; R, reverse; U, unzoned
K-feldspar: M—microcline; O—orthoclase, P—patch; R—rod and bead; Repl.—replacement of plagioclase
Muscovite: Av.—arithmetic mean, Type—A, anhedral replacement product of K-feldspar, plagioclase ± andalusite ± biotite, E, euhedral (primary?) habit.
Biotite: Alt.—type of alteration (C, chlorite; F, fresh; H, hematite, M, muscovite)
Topaz—modal abundance
Andal. (andalusite)—modal abundance.
Tour. (tourmaline)—modal abundance
Fluor. (fluorite)—modal abundance.
*Mineralization*
Type: D—disseminations and fracture fillings, mostly U, F ± Mo ± W, G—greisen ± quartz vein with polymetallic mineralization; P—pegmatite-hosted polymetallic mineralization.
Ref—references: (1) Corey (1991); (2) Ham (1991); (3) Horne (1987), (4) MacDonald & Ham (1992), (5) MacDonald & Horne (1987), (6) Corey (1987).

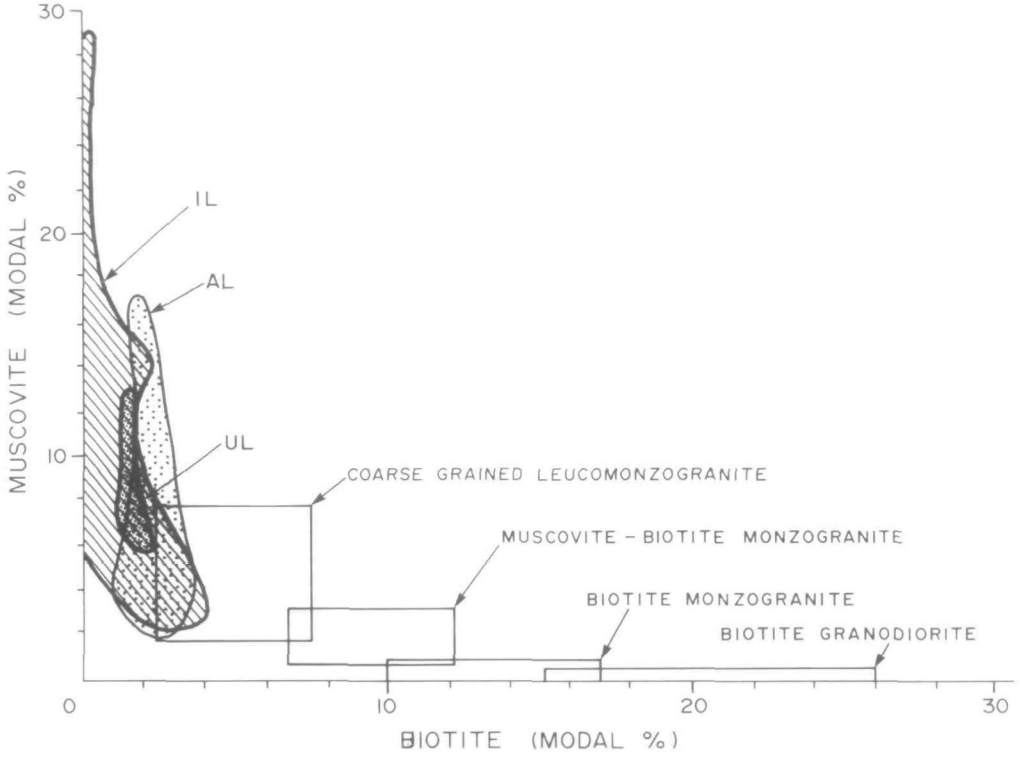


FIG. 3. Comparison of the modal percentages of biotite and muscovite in various rock types of the South Mountain Batholith. AL, associated leucogranite; IL, independent leucogranite; UL, unclassified leucogranite.

representing albitized magmatic oligoclase; modal muscovite contents ranging from 2·5 to 28·5%, with averages of 5·8–16·4% for individual bodies [euhedral primary(?) muscovite is more abundant than anhedral secondary muscovite], significantly higher than the associated leucogranites; modal biotite contents ranging from 0 to 3·9%, with averages of 0·1–1·6% for individual bodies, significantly less than in associated types; muscovite and hematite as the most common alteration products of biotite; andalusite and topaz in amounts up to 0·5%; and trace amounts of fluorite in two of the independent leucogranite bodies.

The unclassified leucogranite rocks from Walsh Brook (WW) typically contain zoned plagioclase ($An_{2-14}$), predominantly anhedral secondary muscovite (5·8–12·4%, av. 8·7%), chloritized biotite (1·0–2·0%, av. 1·5%), trace amounts of andalusite and tourmaline, and no topaz. The unclassified samples are, therefore, petrographically similar to the associated leucogranitic rocks.

In summary, the principal petrographic differences between the two leucogranite types involve the composition and zoning of the plagioclase feldspars, the modal abundance and degree of alteration of biotite, the habit and modal abundance of muscovite, and the modal abundance of minor phases such as andalusite, topaz, and fluorite. Figure 3 shows the mica contents of the leucogranites relative to other rock types in the batholith.

## *Whole-rock geochemistry*

### *Analytical methods*

Analyses for the major oxides and some trace elements (Ba, Rb, Sr, Y, Zr, Nb, Pb, Zn, Cu,

V, and Ga) were done by X-ray fluorescence spectroscopy at the Regional XRF Laboratory at St. Mary's University, Halifax. Other trace elements (Hf, Ta, Sc, La, Th, U, As, and W) were analyzed by instrumental neutron activation analysis, F was determined by specific ion electrode, B by directly coupled plasma atomic emission spectroscopy (DCP-AES), Li by atomic absorption, and Sn by X-ray fluorescence, all at Bondar-Clegg, Ottawa. Ham *et al.* (1989) have described these analytical methods. For most samples, the REE were analyzed by inductively coupled plasma mass spectrometry (ICP-MS) at XRAL in Don Mills, Ontario (lower limits of detection 0·1 ppm for all elements reported, except 0·05 ppm for Eu and Lu). For 16 samples close to or below the detection limit for ICP-MS, the REE were analyzed by neutron activation with the following errors (in ppm) for the lowest reported values based on counting statistics (La $\pm$0·16, Ce $\pm$0·26, Nd $\pm$0·38, Sm $\pm$0·01, Eu $\pm$0·005, Gd $\pm$0·3, Tb $\pm$0·004, Yb $\pm$0·08, and Lu $\pm$0·008); these samples can be identified in Table 2 as they report values for terbium.

Oxygen for isotopic analysis was extracted from silicate minerals by the $BrF_5$ method of Clayton & Mayeda (1963) and quantitatively converted to $CO_2$ over red-hot graphite. The $CO_2$ gas was analyzed using a VG Micromass SIRA-9 mass spectrometer at the University of Western Ontario. The oxygen isotope data are presented in the normal $\delta$ notation relative to Standard Mean Ocean Water (SMOW) (Craig, 1961). An oxygen isotope $CO_2$–$H_2O$ fractionation factor of 1·0412 at 25 °C has been employed in these calculations to calibrate the mass spectrometer reference gas. An average $\delta^{18}O$ value of +9·63 $\pm$ 0·14‰ was obtained for 12 samples of silica standard NBS-28 analyzed during the course of this project.

*Major and trace elements*

Table 2 contains 47 analyses of leucogranitic rocks from the eastern part of the batholith, and Fig. 4 illustrates some of the data. All the chemical plots show a solid line through the means of 57 samples of biotite granodiorite, 44 of muscovite biotite monzogranite, 90 of biotite muscovite monzogranite, and 64 of coarse-grained leucomonzogranite from the entire batholith (Ham *et al.*, 1989). [A similar line on the $\delta^{18}O$ plot is defined by eight unpublished analyses of granodiorite to leucomonzogranite (see Fig. 6 below).] These lines broadly define the magmatic differentiation trend of the batholith (McKenzie & Clarke, 1975; Smith *et al.*, 1986; MacDonald & Clarke, 1991) and will be referred to as the South Mountain magmatic trend. In each part of Fig. 4, the leucogranitic rocks lie at or beyond the most evolved end of the South Mountain magmatic trend, with the independent leucogranite commonly being the most evolved. Although not shown, the leucogranite samples are also lower in $TiO_2$, $FeO_T$, MgO, and CaO than all other rocks in the batholith.

Clarke & Muecke (1985) discussed the major and trace element chemical variation of the South Mountain Batholith in terms of solid–melt, solid–melt–fluid, and solid–fluid reactions. The main processes responsible for chemical differentiation are crystal–melt fractionation (as observed in relatively unaltered rocks), and water–melt–rock or water–rock interaction (as observed in hydrothermally altered rocks). Interpretation of the geochemistry in this section attempts to identify and assess the contributions of magmatic and fluid processes to the formation of the leucogranitic rocks.

Peraluminous granitic rocks owe their high A/CNK values to a combination of source, magmatic, and fluid effects. Silicate melt–silicate crystal equilibria generally constrain A/CNK to values of 1·1–1·2. Figure 4a shows that the leucogranitic rocks generally have A/CNK greater than the magmatic trend, and that the associated leucogranitic rocks skew towards higher $SiO_2$ relative to the independent type. The differences between associated and independent leucogranite compositions might reflect the differences between the styles of fluid interaction, one removing many constituents relative to $SiO_2$, and the other capable of

TABLE 2

*Chemical data for 47 leucogranitic rocks from the eastern South Mountain Batholith; all samples coded LU, and all REE and oxygen isotope data are new, otherwise analyses are from Ham* et al. *(1989)*

| *Sample* | *BB1260-1* | *BB2146-2* | *BB2152-1* | *BB2152-2* | *BBLU-6* | *CL-LU-9* | *CL20-9-3* | *CL20-9-4* | *ED3056* | *ED3057* |
|---|---|---|---|---|---|---|---|---|---|---|
| *Type* | *IL* | *IL* | *IL* | *IL* | *IL* | *AL* | *AL* | *AL* | *AL* | *AL* |
| | | | | | *Major elements* | | | | | |
| $SiO_2$ | 72·05 | 74·77 | 74 90 | 74 27 | 73·30 | 74·40 | 75·24 | 74·78 | 74·70 | 74·06 |
| $TiO_2$ | 0·04 | 0·08 | 0·08 | 0·13 | 0·07 | 0·06 | 0·07 | 0·06 | 0·07 | 0·09 |
| $Al_2O_3$ | 15·38 | 14·22 | 14 16 | 13·88 | 15·00 | 14·50 | 14·00 | 14·27 | 14·45 | 14·30 |
| $Fe_2O_3T$ | 0·95 | 1·38 | 1·33 | 1·79 | 0·81 | 0·37 | 1·16 | 1·22 | 1·03 | 1 20 |
| MnO | 0·03 | 0·03 | 0·03 | 0·04 | 0·01 | 0·01 | 0·04 | 0·04 | 0·04 | 0·05 |
| MgO | 0·72 | 0·69 | 0·66 | 0·84 | 0·21 | 0·28 | 0·80 | 0·72 | 0·78 | 0·85 |
| CaO | 0·40 | 0·21 | 0·26 | 0·31 | 0·19 | 0·52 | 0·30 | 0·30 | 0·28 | 0·33 |
| $Na_2O$ | 4·86 | 3·72 | 3 49 | 3·21 | 3·76 | 4·07 | 3·80 | 3·93 | 3·22 | 3·95 |
| $K_2O$ | 3·50 | 4·37 | 4·23 | 4·38 | 4·12 | 3·79 | 4·48 | 4·06 | 4·28 | 4·17 |
| $P_2O_5$ | 0·54 | 0·29 | 0·34 | 0·33 | 0·27 | 0·42 | 0·28 | 0·32 | 0·32 | 0·38 |
| LOI | 0·67 | 0·71 | 0·82 | 0·70 | 1·54 | 1·54 | 0·51 | 0·60 | 0·70 | 0·80 |
| Total | 98·19 | 100·47 | 98·97 | 98·09 | 99·28 | 99·96 | 100·68 | 100·30 | 99·87 | 100·18 |
| | | | | | *Trace elements* | | | | | |
| Ba | 77 | 27 | 34 | 80 | 170 | 140 | 14 | 12 | 6 | 23 |
| Rb | 845 | 754 | 677 | 691 | 1210 | 590 | 409 | 547 | 497 | 506 |
| Sr | 28 | 11 | 16 | 23 | 10 | nd | 9 | 4 | 3 | 8 |
| Y | 39 | 38 | 37 | 41 | nd | 10 | 24 | 32 | 18 | 19 |
| Zr | 26 | 44 | 42 | 76 | 10 | 10 | 26 | 34 | 37 | 42 |
| Nb | 34 | 27 | 22 | 22 | 30 | 20 | 11 | 13 | 13 | 15 |
| Th | 2·0 | 6·2 | 6·9 | 13·0 | 46·0 | 0·6 | 3·0 | 3·7 | 2·5 | 3 5 |
| Pb | 11 | 22 | 15 | 22 | 4 | 12 | 20 | 16 | 20 | 26 |
| Ga | 30 | 28 | 24 | 24 | na | na | 22 | 22 | 28 | 24 |
| Zn | 64 | 69 | 55 | 69 | 66 | 32 | 51 | 42 | 46 | 65 |
| Cu | nd | nd | nd | nd | 7 | 20 | 4 | nd | nd | nd |
| V | nd | nd | 1 | 5 | 2 | 4 | 3 | nd | 2 | 1 |
| Hf | 2 | 2 | 2 | 3 | 6 | nd | 1 | 1 | 1 | 1 |
| Sc | 2 2 | 2·2 | 2·4 | 2·7 | 6·8 | 16·3 | 2·2 | 2·3 | 2·6 | 2·4 |
| Ta | 14·0 | 7·0 | 6·6 | 5·7 | 2·0 | 6·5 | 2·8 | 3·7 | 3·2 | 3·2 |
| Li | 336 | 324 | 375 | 419 | 490 | 110 | 18 | 59 | 254 | 341 |
| B | 14 | 17 | 38 | 18 | 20 | 20 | 16 | 15 | 30 | 25 |
| F | 4135 | 4200 | 4240 | 3965 | na | na | 675 | 1845 | 1950 | 3200 |
| U | 4·3 | 4·0 | 3 6 | 4 4 | 14·6 | 1·6 | 16·0 | 4·9 | 2·4 | 4·1 |
| W | 8 | 11 | 9 | 7 | 300 | 740 | 5 | 6 | 8 | 10 |
| Sn | 31 | 39 | 26 | 30 | na | na | 18 | 35 | 30 | 48 |
| Au | 3 | nd | nd | 3 | na | na | nd | nd | nd | nd |
| As | 0·7 | 0·9 | 0·9 | 2·5 | nd | 2·0 | 8·4 | 2·0 | 0·7 | 39·0 |
| Sb | 0·3 | 0·1 | nd | 0·1 | 0·4 | nd | nd | nd | 0·2 | 0·2 |
| | | | | | *Rare earth elements* | | | | | |
| La | 1 7 | 4·1 | 5·5 | 11·7 | 0·97 | 2·0 | 2·4 | 2·2 | 2·5 | 3·5 |
| Ce | 3·4 | 8·9 | 11·4 | 25·2 | 2·44 | 2·8 | 4·9 | 4 4 | 5·1 | 7·7 |
| Nd | 1·6 | 4·3 | 5·6 | 13·2 | nd | 1·9 | 2·5 | 2·3 | 2·8 | 4·4 |
| Sm | 0·7 | 1·1 | 1·4 | 3·1 | 0·32 | 0·7 | 0·7 | 0·7 | 0·8 | 1·3 |
| Eu | 0·03 | 0·07 | 0·15 | 0·18 | 0·01 | 0·05 | 0·03 | 0·03 | 0·03 | 0·08 |
| Gd | 0·6 | 0·8 | 1·3 | 2·6 | nd | 0·8 | 0·4 | 0·4 | 0·7 | 1·0 |
| Tb | na | na | na | na | 0·04 | na | na | na | na | na |
| Tm | na | na | na | na | 0·02 | na | na | na | na | na |
| Yb | 0·20 | 0·20 | 0·20 | 0·50 | nd | 0·20 | 0·20 | 0·20 | 0·30 | 0·30 |
| Lu | 0·05 | 0·03 | 0·03 | 0·06 | nd | 0·05 | nd | 0·05 | 0·05 | 0·07 |
| | | | | | *Oxygen isotopes* | | | | | |
| $\delta^{18}O$ | 11·10 | 11·73 | 11·61 | 11·49 | 11·58 | 15·04 | 10·95 | 11·25 | 7·71 | 10·83 |

TABLE 2 (*Continued*)

| *Sample* | *ED3074* | *FC-LU14* | *FC0001* | *FC3000* | *FC3002* | *KR3028* | *KR3028-3* | *KRLU-1M* | *LL1216-4* | *LL1256* |
|---|---|---|---|---|---|---|---|---|---|---|
| *Type* | *AL* | *AL* | *AL* | *AL* | *AL* | *IL* | *IL* | *IL* | *IL* | *IL* |
| | | | | | *Major elements* | | | | | |
| $SiO_2$ | 74·38 | 76·40 | 76·08 | 74 42 | 75·67 | 73·26 | 71·85 | 73·30 | 73·82 | 73·81 |
| $TiO_2$ | 0·07 | 0·14 | 0·10 | 0·11 | 0·16 | 0·05 | 0·03 | 0·06 | 0·06 | 0·06 |
| $Al_2O_3$ | 14·36 | 13·30 | 12·94 | 13·82 | 13·00 | 14·96 | 15·56 | 15·40 | 14·46 | 14·72 |
| $Fe_2O_3T$ | 1·15 | 0·84 | 1 64 | 1·69 | 2·07 | 1·08 | 0·91 | 0·74 | 1·18 | 1·13 |
| MnO | 0·03 | 0·02 | 0·05 | 0·06 | 0·08 | 0·03 | 0·04 | 0·02 | 0·04 | 0·03 |
| MgO | 0·69 | 0·34 | 0·63 | 0·92 | 1·07 | 0·73 | 0·75 | 0·15 | 0·70 | 0·71 |
| CaO | 0·32 | 0·30 | 0·28 | 0·28 | 0·39 | 0·52 | 0·69 | 0·72 | 0·31 | 0·32 |
| $Na_2O$ | 3·29 | 3·25 | 2·70 | 3 41 | 2·98 | 3·67 | 4·14 | 4·00 | 3·55 | 3·97 |
| $K_2O$ | 4·57 | 4 41 | 4·34 | 4·58 | 4·12 | 3·96 | 3·76 | 3·98 | 4·30 | 4·09 |
| $P_2O_5$ | 0·29 | 0·20 | 0·18 | 0·24 | 0·21 | 0·54 | 0·76 | 0·59 | 0·41 | 0·48 |
| LOI | 0·47 | 0·93 | 1·00 | 0·70 | 0·90 | 0·80 | 0·90 | 1·23 | 0·60 | 0·20 |
| Total | 99·62 | 100·13 | 99·94 | 100·23 | 100·65 | 99·60 | 99·39 | 100·19 | 99·43 | 99·52 |
| | | | | | *Trace elements* | | | | | |
| Ba | 12 | 180 | 78 | 84 | 115 | 11 | 28 | 140 | 19 | 15 |
| Rb | 304 | 330 | 248 | 369 | 254 | 819 | 1058 | 1310 | 765 | 896 |
| Sr | 9 | 10 | 18 | 20 | 28 | 7 | 34 | 10 | 14 | 16 |
| Y | 24 | nd | 19 | 25 | 23 | 25 | 28 | 10 | 26 | 25 |
| Zr | 39 | 60 | 63 | 59 | 73 | 32 | 31 | 10 | 39 | 39 |
| Nb | 12 | 20 | 8 | 12 | 11 | 31 | 38 | 30 | 28 | 28 |
| Th | 3·0 | 6·0 | 5·1 | 5·1 | 8·6 | 2·1 | 1 6 | 1·9 | 4·5 | 5·0 |
| Pb | 20 | 12 | 20 | 20 | 21 | 10 | 23 | 12 | 17 | 17 |
| Ga | 21 | na | 19 | 20 | 18 | 31 | 38 | na | 30 | 32 |
| Zn | 29 | 15 | 37 | 30 | 39 | 85 | 107 | 70 | 77 | 87 |
| Cu | 13 | 1 | 2 | nd | nd | nd | nd | 4 | nd | nd |
| V | nd | 10 | 3 | 7 | 7 | nd | 1 | 4 | 3 | 4 |
| Hf | 2 | nd | 2 | 1 | 3 | 1 | 1 | 2 | 1 | 1 |
| Sc | 2 8 | 4·9 | 1·8 | 2·9 | 5·7 | 3·7 | 2·1 | 3 6 | 1·7 | 1·8 |
| Ta | 2·0 | 5·0 | 1·7 | 2·3 | 1·9 | 7·8 | 13·0 | 17·0 | 6·8 | 8·7 |
| Li | 47 | 48 | 62 | 64 | 72 | 488 | 540 | 740 | 417 | 502 |
| B | 15 | 30 | 40 | 45 | 45 | 35 | 30 | 30 | 20 | 25 |
| F | 495 | na | 580 | 405 | 540 | 3950 | 3600 | na | 3300 | 3650 |
| U | 7·6 | 8·7 | 3·4 | 5·0 | 4·2 | 3·8 | 12·0 | 5·8 | 5·2 | 4·6 |
| W | 2 | 1200 | 5 | 2 | 42 | 11 | 8 | 930 | 19 | 8 |
| Sn | 13 | na | 13 | 7 | 9 | 44 | 48 | na | 38 | 41 |
| Au | nd | na | 11 | 3 | 11 | 2 | 2 | na | 2 | 2 |
| As | 4·1 | 5·0 | 7·9 | 1 5 | 1·1 | 1·7 | 1·7 | 2·0 | 1·9 | 2·1 |
| Sb | nd | 0·7 | 0·2 | 0·1 | 0·2 | 0·2 | 0·1 | 1·6 | 0·2 | 0·1 |
| | | | | | *Rare earth elements* | | | | | |
| La | 3·3 | 8·7 | 7·5 | 7·7 | 11·3 | 1·75 | 0·94 | 1·5 | 3·0 | 2·6 |
| Ce | 8·0 | 18·6 | 15·4 | 16·3 | 24·1 | 4·5 | 2·31 | 2·9 | 5·8 | 5·4 |
| Nd | 3·8 | 9·6 | 7·5 | 8 6 | 12·1 | 2·8 | 1·64 | 1·3 | 2·8 | 2·4 |
| Sm | 1·4 | 2 5 | 1·8 | 2·2 | 3·2 | 0·78 | 0·56 | 0·6 | 1·0 | 0·8 |
| Eu | 0·03 | 0·22 | 0·27 | 0·24 | 0·40 | 0·03 | 0·01 | 0·05 | 0·10 | 0·03 |
| Gd | 1·1 | 2·1 | 1·3 | 1·5 | 2 4 | nd | 0·80 | 0·6 | 1·0 | 0·8 |
| Tb | na | na | na | na | na | 0·17 | 0·13 | na | na | na |
| Tm | na | na | na | na | na | 0·04 | 0·04 | na | na | na |
| Yb | 0·30 | 0·80 | 0·40 | 0·60 | 0·80 | 0·28 | 0·20 | 0·10 | 0·20 | 0·30 |
| Lu | 0·06 | 0·09 | 0·07 | 0·12 | 0·15 | 0·04 | nd | 0·03 | 0·07 | 0·06 |
| | | | | | *Oxygen isotopes* | | | | | |
| $\delta^{18}O$ | 11·44 | 13·04 | 12·48 | 12·26 | 13·72 | 11·75 | 11·51 | 11·36 | 10·21 | 11·09 |

TABLE 2 (*Continued*)

| *Sample* | *LL1265* | *LLLU-7C* | *LLLU-8* | *MLE-20* | *MLE-20-2* | *MLE-27* | *MLE18* | *MLE41* | *MLELU-4* | *MLELU-5* |
|---|---|---|---|---|---|---|---|---|---|---|
| *Type* | *IL* | *IL* | *IL* | *IL* | *IL* | *IL* | *IL* | *IL* | *IL* | *IL* |
| | | | | | *Major elements* | | | | | |
| $SiO_2$ | 72 74 | 74·10 | 74·90 | 74·21 | 72·97 | 74·99 | 74·05 | 73·55 | 72 90 | 73·50 |
| $TiO_2$ | 0·06 | 0·08 | 0·08 | 0·08 | 0·02 | 0·04 | 0·09 | 0·04 | 0·04 | 0·06 |
| $Al_2O_3$ | 14·66 | 14 60 | 13·70 | 14·13 | 15·01 | 14·18 | 13 79 | 14·66 | 15·50 | 15·00 |
| $Fe_2O_3T$ | 1·19 | 0·98 | 0·34 | 1 57 | 1 18 | 1·04 | 1·39 | 1·18 | 0·61 | 1·00 |
| MnO | 0·03 | 0·02 | 0·01 | 0·04 | 0·05 | 0·03 | 0·03 | 0·04 | 0·01 | 0·02 |
| MgO | 0·70 | 0·20 | 0·20 | 0·79 | 0·82 | 0·74 | 0·87 | 0·61 | 0·17 | 0·17 |
| CaO | 0·22 | 0·44 | 1·07 | 0·38 | 0·73 | 0·37 | 0·38 | 0·45 | 0·65 | 0·53 |
| $Na_2O$ | 3 57 | 3·65 | 3·90 | 3·41 | 4·69 | 3·87 | 3·19 | 3·38 | 4·76 | 3·86 |
| $K_2O$ | 4·17 | 4·68 | 4·15 | 4·40 | 3·16 | 4·19 | 4·35 | 4·14 | 3·47 | 4·34 |
| $P_2O_5$ | 0·41 | 0·49 | 0·36 | 0·36 | 0·72 | 0·37 | 0·29 | 0·46 | 0·68 | 0·46 |
| LOI | 0·70 | 0·77 | 1·08 | 0·84 | 0·90 | 0·75 | 0·80 | 0·70 | 1·00 | 1·23 |
| Total | 98·45 | 100·01 | 99·79 | 100·21 | 100·25 | 100·57 | 99·23 | 99·21 | 99·79 | 100·17 |
| | | | | | *Trace elements* | | | | | |
| Ba | 23 | 140 | 100 | 42 | 25 | 16 | 47 | 8 | 120 | 80 |
| Rb | 866 | 1050 | 600 | 473 | 613 | 537 | 396 | 601 | 850 | 770 |
| Sr | 20 | nd | nd | 17 | 12 | 6 | 16 | 5 | nd | nd |
| Y | 27 | nd | nd | 27 | 28 | 26 | 19 | 20 | 20 | 6 |
| Zr | 43 | 20 | 10 | 40 | 18 | 26 | 51 | 36 | nd | 20 |
| Nb | 29 | 20 | 10 | 16 | 34 | 16 | 13 | 20 | 20 | 10 |
| Th | 5·5 | 4·9 | 1 9 | 3·6 | 1·5 | 2·4 | 5·0 | 3·1 | 1·5 | 3·0 |
| Pb | 23 | 32 | 8 | 11 | 4 | 9 | 14 | 15 | 4 | 4 |
| Ga | 26 | na | na | 27 | 28 | 24 | 23 | 26 | na | na |
| Zn | 74 | 74 | 13 | 63 | 44 | 32 | 39 | 68 | 35 | 38 |
| Cu | nd | 5 | 10 | 1 | 3 | nd | nd | nd | 5 | 4 |
| V | 1 | 6 | 4 | nd | nd | 1 | 1 | 3 | 2 | 2 |
| Hf | 1 | nd | nd | 1 | 1 | nd | 1 | nd | nd | nd |
| Sc | 1 7 | 1·6 | 3·0 | 1·6 | 1·8 | 2·1 | 1·9 | 2·2 | 2·0 | 3·2 |
| Ta | 8·3 | 13·0 | 6·0 | 3·3 | 8·2 | 3 3 | 2·3 | 5 5 | 17·0 | 7·0 |
| Li | 497 | 440 | 52 | 153 | 92 | 140 | 122 | 329 | 190 | 360 |
| B | 25 | 10 | 10 | 14 | 16 | 19 | 30 | 25 | 10 | 20 |
| F | 3700 | na | na | 1860 | 2065 | 2000 | 1450 | 2900 | na | na |
| U | 5·7 | 9·9 | 2·6 | 2·2 | 1·9 | 2·1 | 4·0 | 2·9 | 1 5 | 2·0 |
| W | 9 | 970 | 830 | 4 | 8 | 7 | 4 | 9 | 950 | 860 |
| Sn | 36 | na | na | 20 | 28 | 23 | 21 | 43 | na | na |
| Au | 2 | na | na | nd | nd | nd | nd | nd | na | na |
| As | 1 4 | 1·0 | 1·0 | 3·1 | 2·5 | 1·4 | 3·7 | 1·6 | 1·0 | 1·0 |
| Sb | 0·2 | 1·4 | 0·5 | 0·1 | nd | nd | 0·1 | 0·2 | 0·5 | 0·8 |
| | | | | | *Rare earth elements* | | | | | |
| La | 2·2 | 2·6 | 1·2 | 5·84 | 1·48 | 1·33 | 5·8 | 1·62 | 0·61 | 1·6 |
| Ce | 4·9 | 6·2 | 2·4 | 10·6 | 3·79 | 3·02 | 12·6 | 3·58 | 1 46 | 3·7 |
| Nd | 2 4 | 2·7 | 1·4 | 6·5 | nd | 1·71 | 6·5 | nd | nd | 2·0 |
| Sm | 0·8 | 0·9 | 0·4 | 1·81 | 0·56 | 0·95 | 2·3 | 0·93 | 0·52 | 1·1 |
| Eu | 0·06 | 0·05 | 0·06 | 0·12 | 0·02 | 0·02 | 0·12 | 0·03 | 0·01 | 0·03 |
| Gd | 0·7 | 1·0 | 0·5 | 2·6 | 1·0 | 1·3 | 2·3 | 1·7 | 0·8 | 1·4 |
| Tb | na | na | na | 0·44 | 0·14 | 0·28 | na | 0·29 | 0·11 | na |
| Tm | na | na | na | 0·08 | 0·03 | 0·04 | na | 0·05 | 0·03 | na |
| Yb | 0·20 | 0·30 | 0·40 | 0·27 | 0·18 | 0·13 | 0·30 | 0·26 | nd | 0·15 |
| Lu | 0·05 | 0·05 | 0·05 | nd | 0·02 | nd | 0·05 | 0·03 | nd | 0·03 |
| | | | | | *Oxygen isotopes* | | | | | |
| $\delta^{18}O$ | 11·31 | 11·53 | 12·66 | 11·63 | 11·24 | 11·69 | 10·18 | 11·30 | 11·44 | 11·82 |

TABLE 2 (*Continued*)

| *Sample* | *MLS-67* | *MLS-68* | *MLS75-22* | *MLW08-3* | *MLW08-4* | *MLW14-2* | *MLW14-3* | *MLW14-4* | *MLWLU-2* | *MLWLU-3* |
|---|---|---|---|---|---|---|---|---|---|---|
| *Type* | *IL* | *IL* | *IL* | *IL* | *IL* | *IL* | *IL* | *IL* | *IL* | *IL* |
| | | | | | *Major elements* | | | | | |
| $SiO_2$ | 74·31 | 73·93 | 73·68 | 72·56 | 72 20 | 73·30 | 73·45 | 73·95 | 74·50 | 73·50 |
| $TiO_2$ | 0·10 | 0·04 | 0·11 | 0·02 | 0·02 | 0·07 | 0·08 | 0·05 | 0·07 | 0·08 |
| $Al_2O_3$ | 14·05 | 14·66 | 14·33 | 15 29 | 15 50 | 14·99 | 14·24 | 14·43 | 14·50 | 15·00 |
| $Fe_2O_3T$ | 1·50 | 1·10 | 1·36 | 1·26 | 1·15 | 1·25 | 1·08 | 1·06 | 0·70 | 0·65 |
| MnO | 0·03 | 0·03 | 0·04 | 0·04 | 0·04 | 0·04 | 0·03 | 0·03 | 0·01 | 0·02 |
| MgO | 0·81 | 0·75 | 0·80 | 0·66 | 0·63 | 0·84 | 0·77 | 0·71 | 0·22 | 0·21 |
| CaO | 0·30 | 0·28 | 0·35 | 0·57 | 0·60 | 0·50 | 0·30 | 0·35 | 0·41 | 0·63 |
| $Na_2O$ | 3·25 | 4 68 | 3·60 | 3·97 | 4·20 | 3·69 | 4·02 | 3·29 | 3·91 | 3·64 |
| $K_2O$ | 4·57 | 3·88 | 4·37 | 3·46 | 3·48 | 3·82 | 4·35 | 4·30 | 4·51 | 4·09 |
| $P_2O_5$ | 0·28 | 0·41 | 0·34 | 0·69 | 0·71 | 0·48 | 0·36 | 0·35 | 0·34 | 0·52 |
| LOI | 0·70 | 0·80 | 0·60 | 0·91 | 0·81 | 1·11 | 0·87 | 0·77 | 1·00 | 1·47 |
| Total | 99·90 | 100·56 | 99·58 | 99·43 | 99·34 | 100·09 | 99·55 | 99·29 | 100·17 | 99·81 |
| | | | | | *Trace elements* | | | | | |
| Ba | 77 | 11 | 70 | 14 | 24 | 15 | 54 | 33 | 110 | 110 |
| Rb | 373 | 498 | 406 | 745 | 737 | 650 | 497 | 539 | 690 | 840 |
| Sr | 17 | 5 | 17 | 21 | 24 | 10 | 10 | 7 | nd | nd |
| Y | 23 | 25 | 26 | 34 | 36 | 34 | 27 | 25 | nd | 10 |
| Zr | 60 | 23 | 50 | 42 | 16 | 34 | 33 | 23 | 10 | 30 |
| Nb | 12 | 22 | 18 | 29 | 28 | 30 | 16 | 18 | 20 | 30 |
| Th | 5·2 | 1·8 | 6 2 | 1·7 | 1·1 | 2·1 | 4·4 | 1·9 | 2·0 | 2·5 |
| Pb | 20 | 7 | 12 | 14 | 8 | 12 | 13 | 8 | 12 | nd |
| Ga | 22 | 28 | 23 | 34 | 32 | 31 | 24 | 24 | na | na |
| Zn | 54 | 49 | 40 | 75 | 77 | 51 | 36 | 27 | 25 | 33 |
| Cu | 1 | nd | nd | 2 | nd | 8 | nd | 1 | 3 | 7 |
| V | 3 | nd | 9 | nd | 7 | nd | 2 | nd | 4 | nd |
| Hf | 2 | 1 | 3 | 4 | nd | nd | 1 | nd | nd | nd |
| Sc | 2·3 | 2·8 | 2·9 | 1·7 | 1·4 | 5·4 | 2·1 | 2·2 | 2·7 | 5·9 |
| Ta | 2·1 | 3·4 | 4·4 | 5·0 | 4·1 | 5·9 | 3·0 | 4 2 | 6·0 | 11·0 |
| Li | 105 | 98 | 111 | 205 | 205 | 173 | 134 | 97 | 130 | 180 |
| B | 18 | 20 | 23 | 12 | 12 | 15 | 13 | 12 | 20 | 10 |
| F | 1155 | 1685 | 1235 | 2645 | 2705 | 2100 | 1500 | 1640 | na | na |
| U | 3·6 | 5·8 | 7·0 | 3·8 | 2·6 | 2·5 | 2·2 | 1·7 | 1·6 | 2·8 |
| W | 4 | 5 | 6 | 8 | 8 | 8 | 5 | 6 | 930 | 1000 |
| Sn | 18 | 22 | 18 | 26 | 27 | 29 | 25 | 23 | na | na |
| Au | nd | nd | nd | nd | 6 | nd | nd | nd | na | na |
| As | 1·0 | 2·4 | 4·0 | 3·8 | 4·2 | 2·7 | 2·0 | 3 2 | 5·0 | 2·0 |
| Sb | nd | nd | nd | 0·1 | 0·1 | 0·1 | 0·2 | nd | 0·5 | 0·6 |
| | | | | | *Rare earth elements* | | | | | |
| La | 5·7 | 1·0 | 8·7 | 1·12 | 0·54 | 2·02 | 5·3 | 2·69 | 1·8 | 2·4 |
| Ce | 15·3 | 2·3 | 18·1 | 4·02 | 1 53 | 5·41 | 12·2 | 5·62 | 4·2 | 5·4 |
| Nd | 6·5 | 2·3 | 9·6 | nd | nd | 4·24 | 6·9 | 3·20 | 2·6 | 2·6 |
| Sm | 2·5 | 0·8 | 2·3 | 1·02 | 0·61 | 0·86 | 1 72 | 0·92 | 0·7 | 1·0 |
| Eu | 0·13 | 0·01 | 0·24 | 0·03 | 0·02 | 0·02 | 0·08 | 0·04 | 0·04 | 0·05 |
| Gd | 1·3 | 1·2 | 2·0 | 1·6 | 1·4 | 1·3 | 1·8 | 1·4 | 1·0 | 1·2 |
| Tb | 0·46 | 0·25 | na | 0·28 | 0·22 | 0·24 | 0·32 | 0·22 | 0·18 | na |
| Tm | 0·08 | 0·04 | na | 0·04 | 0·04 | 0·06 | 0·08 | 0·05 | 0·06 | na |
| Yb | 0·32 | 0·17 | 0·30 | 0·13 | nd | 0·38 | 0·40 | 0·24 | 0·35 | 0·30 |
| Lu | 0·04 | nd | 0·06 | nd | nd | 0·03 | 0·05 | 0·02 | 0·04 | 0·05 |
| | | | | | *Oxygen isotopes* | | | | | |
| $\delta^{18}O$ | 11·35 | 10·95 | 11·01 | 11·29 | 11·25 | 12·06 | 11·04 | 11·35 | 11·19 | 11·71 |

TABLE 2 (*Continued*)

| *Sample* | *TA0100* | *TA3120* | *TALU-12A* | *WW2026* | *WW2027* | *WW2086* | *W2086-1* |
|---|---|---|---|---|---|---|---|
| *Type* | *AL* | *AL* | *AL* | *UL* | *UL* | *UL* | *UL* |
| | | | *Major elements* | | | | |
| $SiO_2$ | 75·08 | 74·85 | 74·40 | 72·81 | 73·01 | 73·93 | 73·19 |
| $TiO_2$ | 0·05 | 0·05 | 0·11 | 0·19 | 0·15 | 0·18 | 0·14 |
| $Al_2O_3$ | 14·23 | 14·24 | 14·10 | 15·07 | 14·70 | 14·98 | 14·69 |
| $Fe_2O_3T$ | 1·21 | 1·20 | 1·05 | 1·46 | 1 43 | 1·58 | 1·25 |
| MnO | 0·08 | 0·06 | 0·04 | 0·03 | 0·03 | 0·03 | 0·03 |
| MgO | 0·54 | 0·56 | 0·29 | 0·85 | 0·77 | 1·10 | 0·98 |
| CaO | 0·28 | 0·31 | 0·43 | 0·38 | 0·37 | 0·39 | 0·33 |
| $Na_2O$ | 3 75 | 3·85 | 3 54 | 3·14 | 3·41 | 3·74 | 3·60 |
| $K_2O$ | 4·38 | 4·20 | 4·74 | 4·69 | 4·36 | 4·64 | 4·93 |
| $P_2O_5$ | 0·17 | 0·26 | 0·24 | 0·31 | 0·32 | 0·30 | 0·30 |
| LOI | 0·60 | 0·70 | 1·00 | 0·90 | 1·00 | 0·60 | 1·10 |
| Total | 100·37 | 100·28 | 99·94 | 99·83 | 99·55 | 101 47 | 100·54 |
| | | | *Trace elements* | | | | |
| Ba | 28 | 10 | 130 | 226 | 216 | 280 | 218 |
| Rb | 327 | 424 | 520 | 188 | 194 | 207 | 207 |
| Sr | 14 | 7 | nd | 49 | 43 | 55 | 40 |
| Y | 21 | 18 | 20 | 14 | 12 | 15 | 15 |
| Zr | 42 | 40 | 40 | 70 | 60 | 66 | 57 |
| Nb | 9 | 11 | 10 | 9 | 10 | 10 | 10 |
| Th | 4·3 | 3·7 | 5·2 | 5·5 | 4·8 | 4·7 | 3·5 |
| Pb | 26 | 15 | 8 | 19 | 36 | 10 | 9 |
| Ga | 19 | 22 | na | 18 | 21 | 20 | 19 |
| Zn | 34 | 37 | 34 | 58 | 190 | 26 | 22 |
| Cu | 1 | nd | 2 | nd | 2 | nd | nd |
| V | 3 | 3 | 6 | 8 | 11 | 8 | 7 |
| Hf | 1 | 1 | 2 | 2 | 1 | 2 | 2 |
| Sc | 3·1 | 2·6 | 4·7 | 2·5 | 2·9 | 3 2 | 3·0 |
| Ta | 2·4 | 3·2 | 5·0 | 1·4 | 1·4 | 1·3 | 1·4 |
| Li | 172 | 104 | 160 | 23 | 22 | 36 | 19 |
| B | 20 | 30 | 20 | 100 | 50 | 50 | 40 |
| F | 560 | 1050 | na | 245 | 310 | 320 | 335 |
| U | 9·1 | 5·4 | 11·5 | 2 5 | 3·6 | 2·5 | 7·3 |
| W | 4 | 6 | 900 | 4 | 5 | 3 | 4 |
| Sn | 22 | 28 | na | 4 | 14 | 14 | 12 |
| Au | 12 | 9 | na | 23 | 11 | 20 | 4 |
| As | 1·2 | 4·7 | 1·0 | 6·3 | 1·9 | 4·1 | 4·5 |
| Sb | 0·1 | 0·1 | 1·0 | nd | 0·1 | nd | nd |
| | | | *Rare earth elements* | | | | |
| La | 4·0 | 3·5 | 5·6 | 9·2 | 8·2 | 10·4 | 8·3 |
| Ce | 10·1 | 8·1 | 13·0 | 19·0 | 17·0 | 21 6 | 16·9 |
| Nd | 4·6 | 4·1 | 7 3 | 11 1 | 9·1 | 11·7 | 9·3 |
| Sm | 1·7 | 1·4 | 2·1 | 3·2 | 2·5 | 3·0 | 2·5 |
| Eu | 0·06 | 0·12 | 0·17 | 0·53 | 0·47 | 0·65 | 0·53 |
| Gd | 1·2 | 0·9 | 1·6 | 2·3 | 2·3 | 2·5 | 2·1 |
| Tb | na | na | na | na | na | na | na |
| Tm | na | na | na | na | na | na | na |
| Yb | 1·0 | 0·7 | 0·9 | 0·4 | 0·5 | 0·7 | 0·6 |
| Lu | 0·14 | 0·14 | 0·12 | 0·10 | 0·10 | 0·13 | 0·09 |
| | | | *Oxygen isotopes* | | | | |
| $\delta^{18}O$ | 10·71 | 11·36 | 11·28 | 11·62 | 10·82 | 11·72 | 10·03 |

na, not analyzed; nd, not detected.

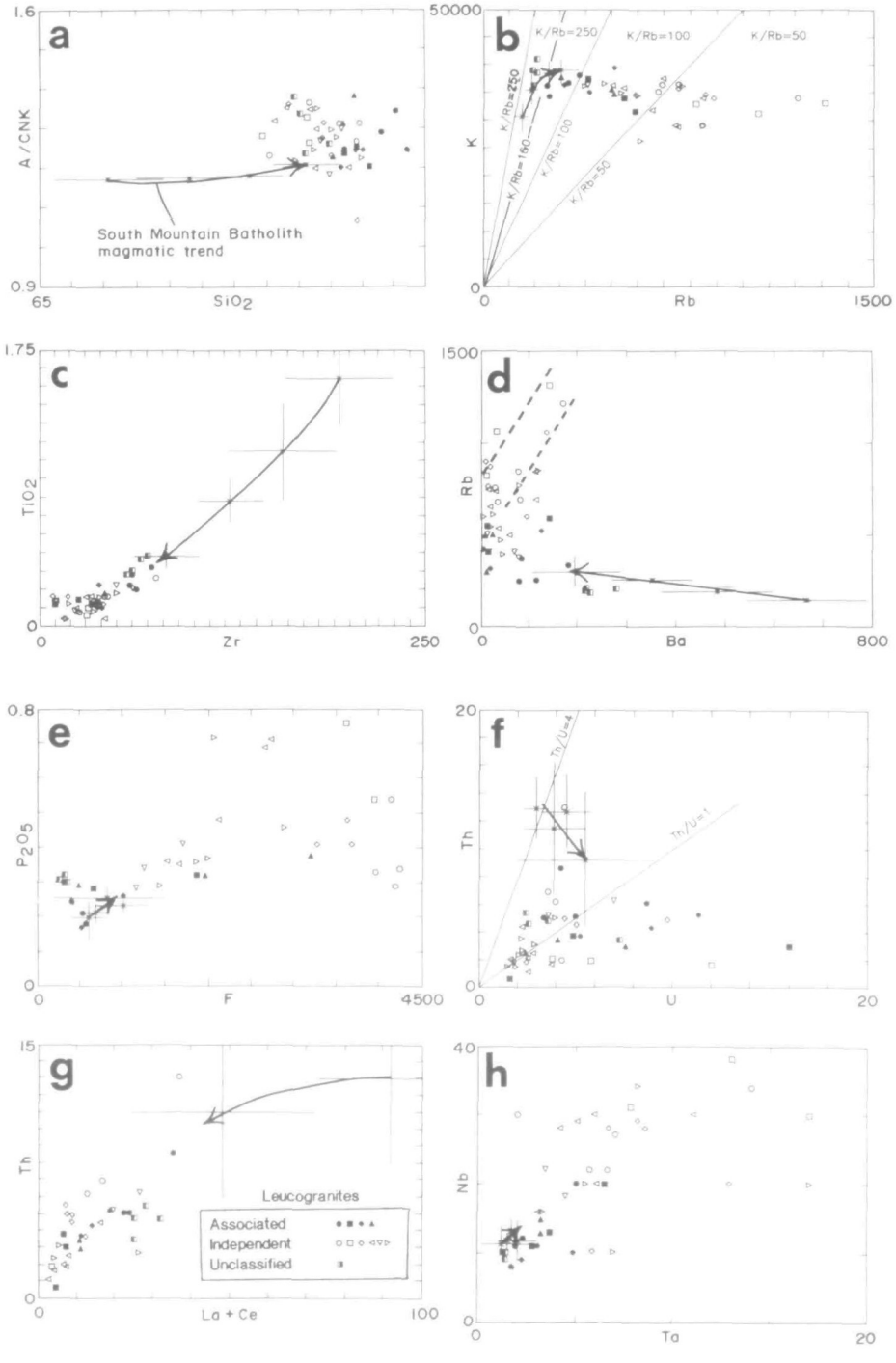


FIG. 4. Chemical variation diagrams for major and trace elements. The heavy line on each graph is the South Mountain magmatic trend; the arrowheads indicate the direction of increasing differentiation dominated by crystal–melt separation. Error bars represent 1 S.D. from the means for the average granodiorite, biotite–muscovite monzogranite, muscovite biotite monzogranite, and coarse-grained leucomonzogranite. (Symbols are keyed to sampling localities shown in Fig. 1: AL, associated leucogranite; IL, independent leucogranite; UL, unclassified leucogranite.)

removing $SiO_2$, respectively. Late quartz–fluorite veins, episyenites, and silicified rocks occurring elsewhere in the batholith may demonstrate the mobility of silica (Logothetis, 1984). The unclassified leucogranite samples are similar to the independent type. The question raised by these variations is whether silicate melt–silicate crystal equilibria can produce such high values of $SiO_2$ and A/CNK.

Critical to our understanding of the processes operating in the late stages of the batholith is the K/Rb variation (Fig. 4b). Taylor (1965) and Shaw (1968) claimed that K/Rb ratios $>160$ indicate control by crystal–melt equilibria, and that lower values are unattainable by crystal–melt processes and reflect involvement of an aqueous fluid phase which stabilizes abundant primary or secondary muscovite with low K/Rb. By this criterion, all the South Mountain leucogranites show the effects of some fluid interaction, and the independent type more than the associated type. Supporting evidence for fluid interaction includes: (1) the presence in some rocks of minerals such as pure albite and topaz; (2) the intimate association of miarolitic cavities and pegmatitic segregations with the independent leucogranites; (3) pronounced enrichment or depletion profiles for many elements in host granitic rocks near veins and greisen zones (Logothetis, 1984); (4) REE depletion during greisenization (Farley, 1978); (5) pronounced differences of interelement correlation between the magmatic and fluid-dominated rocks (MacDonald & Clarke, 1991); and (6) U–F–$P_2O_5$ enrichment in the Millet Brook uranium deposit (Chatterjee *et al.*, 1985).

Figure 4c shows that, in terms of Ti–Zr variation, most of the leucogranitic rocks lie along the extension of the magmatic trend. This relationship suggests a single controlling process such as crystal–melt fractionation of biotite and zircon. If fluid-dominated processes are involved, their effects are co-linear.

The Ba–Rb magmatic trend in Fig. 4d reflects fractional crystallization of alkali feldspar. Again, the two types of leucogranite generally behave differently. The associated and unclassified leucogranite samples lie close to the known magmatic trend, whereas the independent leucogranite group extends to high Rb. The dashed lines show some anomalous positive correlations of Ba–Rb within specific independent leucogranitic bodies. If fluids are responsible for the Ba–Rb variations, then the process affecting the independent leucogranite bodies stabilizes both Ba (in K-feldspar) and Rb (in muscovite), whereas the process affecting the associated type does not.

Figure 4e shows a general positive correlation between F and $P_2O_5$ in the leucogranite population and, more significantly, compositional variation that extends well beyond the magmatic trend. In general, the associated and unclassified leucogranites plot closer to the magmatic trend than the independent type. Although fluorine and phosphorus may form soluble complexes in peraluminous silicate melts (London *et al.*, 1988; Montel *et al.*, 1988), both of these elements also correlate positively with Rb (associated leucogranite group F–Rb Spearman $r_s=0{\cdot}66$, P–Rb $r_s=0{\cdot}74$; independent leucogranite group F–Rb $r_s=0{\cdot}26$, P–Rb $r_s=0{\cdot}48$). If positive correlation with Rb signifies control by a fluid, then the F–P relationships in associated leucogranite bodies suggest greater influence in the associated than in the independent types.

Figure 4f shows a magmatic trend of increasing U and decreasing Th (owing to monazite fractionation; see also Fig. 4g). By contrast, almost all the leucogranitic samples have low Th and highly variable U, but distinctions between the various types are not clear. In fact, a weak positive correlation (Spearman $r_s=0{\cdot}37$) exists between U and Th in the whole population, but not in the individual bodies. The low concentrations of Th suggest the destruction of a Th-bearing phase in the associated leucogranite, and perhaps also the independent type, and its positive correlation with the LREE (Fig. 4h) suggests that this phase is monazite. Monazite crystallization and removal in the magmatic stage might decrease the $\Sigma$LREE and

($La_N/Sm_N$), and its dissolution and removal by a fluid phase could extend these trends. If the Th of monazite is removed by the fluids, apparently the $P_2O_5$ is not; this phosphorus remains in apatite, triplite, amblygonite, and feldspars (Logothetis, 1984). The difference in behaviour of Th and U, as measured by the Th/U ratios, presumably reflects differences in valence states and solubilities in fluids. The correlation of U and $\delta^{18}O$ in the associated leucogranite is weak ($r_s = -0{\cdot}23$), but may have some local economic significance (see below).

Decreasing (La + Ce) and Th in the South Mountain magmatic trend (Fig. 4g) reflect fractional crystallization of monazite. The leucogranite samples plot on an extension of this trend but are separate from it, so may or may not reflect the same process.

The geochemical coherence of $Ta^{6+}$ ($r = 0{\cdot}64$ Å) and $Nb^{6+}$ ($r = 0{\cdot}64$ Å) in magmatic rocks is well established (Parker & Fleisher, 1968; Kovalenko *et al.*, 1977). Ta–Nb relationships (Fig. 4g) show that the associated and unclassified leucogranites deviate only slightly from the restricted variation shown by the magmatic suite, whereas the independent type generally has higher Ta and Nb. Mean Nb/Ta values in the magmatic suite are: biotite granodiorite, 10·1; muscovite biotite monzogranite, 7·8; biotite muscovite monzogranite, 7·5; coarse-grained leucomonzogranite, 5·9. In contrast, the leucogranites have the following Nb/Ta ratios: associated leucogranite, $4{\cdot}2 \pm 1{\cdot}1$; independent leucogranite, $4{\cdot}3 \pm 2{\cdot}5$; unclassified leucogranite, $7{\cdot}1 \pm 0{\cdot}5$. The associated and independent leucogranites have generally lower Nb/Ta values than the magmatic rocks, and the large standard deviation from the mean shown by the independent type suggests significant decoupling of these normally coherent elements. Clearly, Nb/Ta values in the unclassifed leucogranite bodies differ significantly from the other two types; they resemble the intermediate part of the magmatic trend. The strong enrichments of Ta and Nb relative to the South Mountain magmatic trend, and their dispersion in the independent leucogranites, suggest control by fluids. The enrichment suggests stabilization of wolframite, as in many greisens of this batholith, or perhaps tapiolite, and the dispersion might be a function of temperature, fluid composition (especially high F; Wang *et al.*, 1982), and $f_{O_2}$.

*Rare earth elements*

Figure 5 shows REE patterns for early magmatic rocks of the batholith, and for the leucogranite types. The early magmatic rocks (Fig. 5a) have high ΣREE, show approximately the same degree of fractionation for the LREE as the HREE, and have small Eu/Eu* anomalies [where Eu* = (Sm + Gd)/2]. From early granodiorites to later leucomonzogranites, the magmatic suite shows decreases in ΣREE and Eu/Eu*. The unclassified leucogranite type (Fig. 5b) compares closely with the most evolved end of the magmatic range with low ΣREE, smooth patterns, and small Eu/Eu*. By contrast, many of the patterns of the associated leucogranite (Fig. 5c) overlap with the magmatic range, but they also extend to lower ΣREE and lower Eu/Eu* values. More importantly, Figs. 5e–h show that the REE patterns of the associated leucogranite samples are very similar to those of their fine-grained leucomonzogranite hosts. Figures 5d and 5i–n show that the REE contents of the independent leucogranitic rocks overlap with those of the associated type as follows (independent, associated): $La_N/Sm_N$—$1{\cdot}54 \pm 0{\cdot}52$, $1{\cdot}88 \pm 0{\cdot}34$; Eu/Eu*—$0{\cdot}15 \pm 0{\cdot}10$, $0{\cdot}24 \pm 0{\cdot}14$; $Gd_N/Yb_N$—$4{\cdot}6 \pm 2{\cdot}2$, $2{\cdot}0 \pm 0{\cdot}7$. Relative to the associated leucogranite, the independent leucogranite bodies tend towards less fractionated LREE patterns, lower Eu/Eu* values, and more fractionated and highly variable HREE patterns.

The similarity in REE patterns for the associated leucogranite bodies and their fine-grained leucomonzogranite hosts (Figs. 5e–h) demonstrate that at least some REE-bearing minerals were relatively stable during hydrothermal alteration. The same LREE mobility

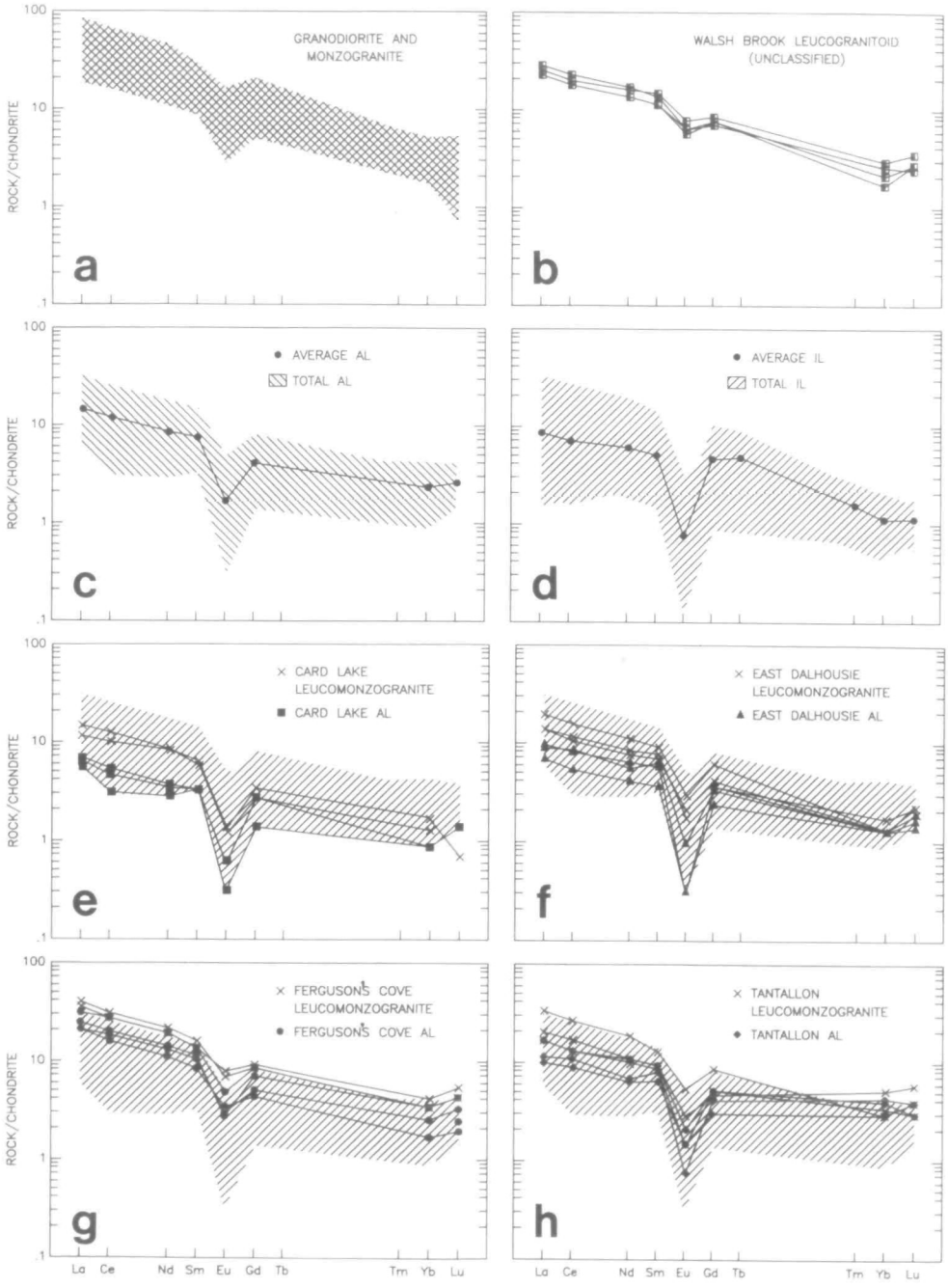


FIG. 5 (a–h)

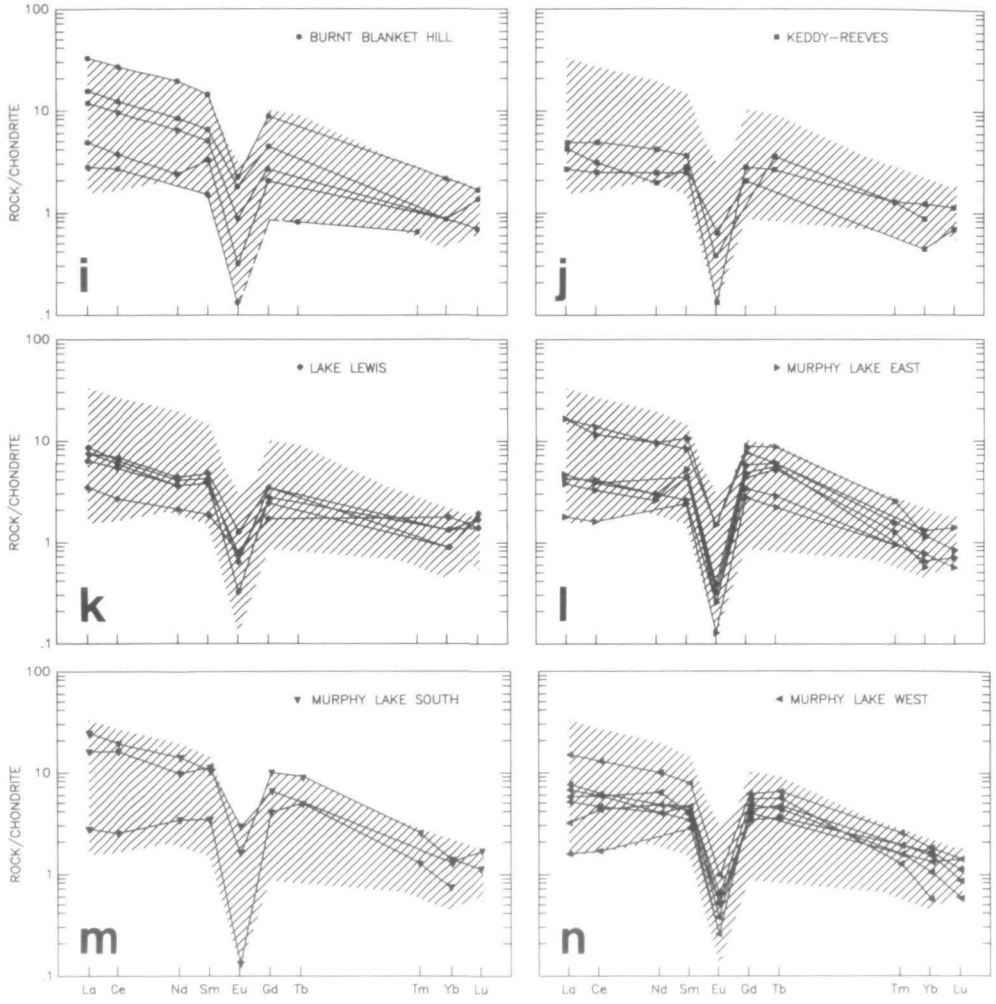


FIG. 5. Rare earth element variation diagrams. (a)–(d) Averages and ranges for the South Mountain Batholith and the three types of leucogranitic rocks. (e)–(h) Host leucomonzogranitic rocks and their associated leucogranites (shaded area is range of associated leucogranite compositions in the South Mountain Batholith). (i)–(n) Independent leucogranite bodies (shaded area is range of independent leucogranite compositions in the South Mountain Batholith).

occurs in almost all the independent leucogranite samples, but in addition, the HREE fractionation is generally greater and more variable. The higher temperatures, more effective physical contact of fluid and melt, and potential formation of HREE-F melt (Ponader & Brown, 1989) and aqueous (Öhlander *et al.*, 1989) complexes may account for the marked differences between HREE in the independent and associated groups.

### *Oxygen isotopes*

The whole-rock $\delta^{18}O$ values of 47 samples of leucogranitic rocks from the batholith range from +7·71 to +15·04‰, and average +11·44 ± 1·01‰ (1$\sigma$) (Table 2), with most values (42 of 47) lying between $\delta^{18}O = +10{\cdot}15$ and +12·70‰ [average +11·38 ± 0·49 (1$\sigma$)]. Averages

by leucogranitic type are: associated ($n=13$) $+11{\cdot}70\pm1{\cdot}75$; independent ($n=30$) $+11{\cdot}38\pm0{\cdot}47$; unclassified ($n=4$) $+11{\cdot}05\pm0{\cdot}79$. These values are similar to those ($+10{\cdot}1$ to $+12{\cdot}0$‰) reported for the South Mountain Batholith as a whole (Longstaffe *et al.*, 1980; Kontak *et al.*, 1988), and they reflect the dominance of $^{18}O$-rich supracrustal protolith(s) for the parental granitic magmas.

Figure 6a illustrates the relationship between whole-rock $\delta^{18}O$ values and $SiO_2$ for 47 samples of leucogranitic rocks (Table 2). The magmatic trend intersects the cluster of data for the leucogranitic rocks in a fashion similar to that observed for the other chemical variables (e.g., Fig. 4). Two other features are also apparent on this diagram. First, the associated

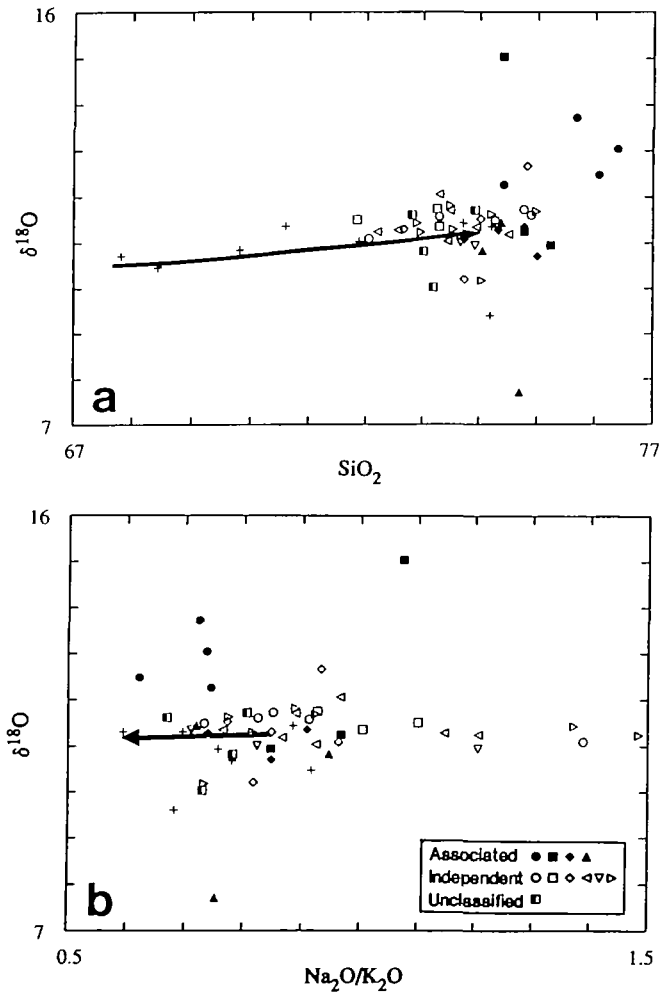


FIG. 6. Variation in whole-rock $\delta^{18}O$ values (in ‰ relative to SMOW). Arrows as in Fig. 3; +, samples used to define the magmatic trend. (a) $\delta^{18}O$–$SiO_2$, showing approximate magmatic trend in the South Mountain Batholith and the field of leucogranitic rocks skewed toward high silica values. (b) $\delta^{18}O$–$Na_2O/K_2O$, showing that increasing $Na_2O/K_2O$ (albitization) of the independent leucogranites did not affect their oxygen isotopic composition, whereas the alteration responsible for producing some of the associated leucogranites did affect theirs.

leucogranite samples include a group that have high values for both $SiO_2$ and $\delta^{18}O$ (> +12‰). Other granitic rocks with very high $\delta^{18}O$ values (+13 to +15‰) occur in the batholith, and some of them are associated with uranium mineralization (Chatterjee & Strong, 1985). Second, a few leucogranitic samples trend toward anomalously low $\delta^{18}O$ values, and even lower values occur at a few other localities in the South Mountain Batholith (Longstaffe *et al.*, 1980; Kontak *et al.*, 1988). Lowering of bulk $\delta^{18}O$ values in granitoid rocks is a common effect of post-crystallization, hydrothermal alteration by meteoric water, but confirmation of such a process requires isotopic analysis of individual minerals. If such alteration has occurred, coexisting minerals will commonly be grossly out of high-temperature oxygen-isotope equilibrium, and the feldspars, in particular, will be anomalously depleted in $^{18}O$ (Taylor, 1978).

Figure 6b shows that the $\delta^{18}O$ values in the independent leucogranite samples (+10·5 to +12·0‰) are generally independent of $Na_2O/K_2O$ variations. Many associated leucogranite samples also follow this pattern; however, some with $Na_2O/K_2O$ in the range 0·6–0·8 scatter to both higher and lower $\delta^{18}O$ values. Variations in the alkali ratio probably represent fractional crystallization (generally towards lower $Na_2O/K_2O$), followed by closed-system(?) metasomatic albitization (towards higher $Na_2O/K_2O$). If so, the anomalously high and low $\delta^{18}O$ values require a different explanation. The $^{18}O$-rich ($\delta^{18}O$ = 12·3–13·7‰) and $SiO_2$-rich associated leucogranite samples from Ferguson's Cove may be the products of deuteric alteration and oxygen-isotope re-equilibration between the rock and magmato-metamorphic waters ($\delta^{18}O \sim +11{\cdot}3$‰). These $^{18}O$-rich samples at Ferguson's Cove, immediately adjacent to the Meguma Group country rocks ($\delta^{18}O$ values of +11·7 to +12·5‰; Longstaffe *et al.*, 1980), represent a source of $^{18}O$-rich fluids. Perhaps, also, these same high-temperature fluids also transported silica into the leucogranitic rocks, or leached feldspar from them. To reach the highest $\delta^{18}O$ value (+13·7‰) would require a temperature of ~430 °C, assuming complete isotopic exchange in a system dominated by such magmato-metamorphic fluids. This temperature estimate uses the alkali feldspar–water oxygen-isotope geothermometer of O'Neil & Taylor (1967), on the assumption that the bulk isotopic composition of the granitoid rock can be approximated by the $\delta^{18}O$ value of its feldspar (Taylor, 1968). If only some of the minerals participated in the subsolidus isotopic exchange, even lower temperatures would be indicated. In addition, the associated leucogranite with the highest $\delta^{18}O$ value (CL-LU9 from Card Lake, +15·0‰) has much higher $Na_2O/K_2O$ than the associated leucogranite samples from Ferguson's Cove. Also, relative to almost all the other analyzed samples, it is also high in Sc (16 ppm) and low in U (1·6 ppm). This sample location is close to the Millet Brook uranium deposit, where the host rocks also show high $\delta^{18}O$ values (Chatterjee & Strong, 1985), so the possibility of a genetic relationship between the $\delta^{18}O$ composition and uranium mineralization warrants further investigation.

Open-system hydrothermal alteration dominated by low $\delta^{18}O$ meteoric water also provides the simplest explanation for the associated leucogranite samples with anomalously low $\delta^{18}O$ values. Specifically, sample ED3056 ($\delta^{18}O$ = +7·7‰) occurs near a major fault zone that may have been a conduit for surface-derived water. As before, the temperature of such water–rock interactions can be estimated for a fluid-dominated system by the alkali feldspar–water geothermometer (O'Neil & Taylor, 1967; Taylor, 1968). For example, if the initial $\delta^{18}O$ leucogranite and the water values were +11·3‰ and 0‰, respectively, and if the rock value was +7·7‰ after equilibration, then the alteration temperature would be ~250 °C, but if the meteoric waters had a lower $\delta^{18}O$ value (for example, −10‰), then the temperature of alteration would have been even lower (~100 °C).

At low temperatures, however, K-feldspar appears to be more reactive than other minerals, and also preferentially exchanges oxygen isotopes with meteoric water during

hydrothermal water–rock interaction (Taylor, 1968, 1978). For example, the K-feldspar in sample ED3056 ($\delta^{18}O = +7{\cdot}7‰$) has an unusual reaction rim of sericite. If this K-feldspar formed ~25% of the rock, and if the bulk depletion of $^{18}O$ were accomplished by alteration of K-feldspar only, then an alteration temperature of ~250 °C would be indicated for exchange with meteoric water of $\delta^{18}O = -10‰$. Confirmation of this possibility, however, requires isotopic analysis of separated minerals.

*Summary of the geochemistry*

In most of the chemical diagrams (Figs. 4–6) the leucogranitic rocks form an extension of the South Mountain magmatic trend towards 'more evolved' compositions. But is this relationship controlled by magmatic (silicate melt–silicate crystal) processes? The key plot is the K–Rb diagram (Fig. 4b), which shows conclusively that, for most of the associated leucogranitic rocks, and all of the independent ones, the very low K/Rb values can only have been reached by fluid interaction. In this light, the high A/CNK, $Na_2O/K_2O$, $P_2O_5$, F, and $Gd_N/Yb_N$, the low Ti, Zr, Ba, and Th, and the erratically variable U and $\delta^{18}O$ values can all be viewed as effects of different styles of fluid interaction. Chatterjee (1992) also found evidence of some Sr and Pb isotopic re-equilibration in samples with K/Rb < 160.

The positions of the associated and independent leucogranite compositions relative to the magmatic rocks on the chemical plots may indicate that fluids had more influence on the final composition of the independent leucogranite than on the associated type. On the basis of the different field relations of these two types, and their different geochemical characteristics, two kinds of fluid interaction may have been involved: (1) subsolidus hydrothermal alteration, and (2) late-stage fluid–magmatic interaction. The transition in the field from associated leucogranite to host leucomonzogranite, and the similarity of at least some their high field strength elements (HFSE; Nb, Ta, P, and REE), suggest that varying, but moderate, degrees of water–rock interaction may account for the associated compositions. The independent leucogranite might just represent an intensification of the same process; however, the field association of independent leucogranites with pegmatites, the markedly lower K/Rb ratio, the strong fractionation of HREE (perhaps by complexing with fluorine; Muecke & Clarke, 1981), and approximately constant $\delta^{18}O$ all suggest that late-stage fluid–magmatic processes were involved.

Compositional overlap between associated and independent leucogranites exists for every element, but if $SiO_2$ is >75%, or if the $\delta^{18}O$ value is outside the range 10·0–12·8‰, the sample is probably of the associated variety. On the other hand, diagnostic independent leucogranite chemical characteristics include $Na_2O > 4{\cdot}10\%$, $K_2O < 3{\cdot}75\%$, $P_2O_5 > 0{\cdot}45\%$, F > 3500 ppm, Rb > 600 ppm, Ta > 7 ppm, Nb > 20 ppm, Li > 350 ppm, and $Gd_N/Yb_N > 4$. This simple chemical screen for independent leucogranites excludes about a third of the independent samples, i.e., those that overlap with the associated ones. Also, two- and three-element discriminant function analysis (e.g., for $P_2O_5$–Rb, or $La_N/Sm_N$–Eu/Eu*–$Gd_N/Yb_N$) similarly tends to misclassify approximately the same number of independent as associated samples. These chemical distinctions, based on the eastern part of the South Mountain Batholith, may not apply elsewhere; much depends on the composition of the silicate melt at the time water-saturation is reached.

The whole-rock $\delta^{18}O$ values, on their own, suggest that the independent leucogranite bodies formed essentially as closed systems, and at temperatures sufficiently high that little or no isotopic fractionation of oxygen occurred. By contrast, the associated leucogranite data, including those showing markedly higher and lower $\delta^{18}O$ values than the main magmatic trend, suggest that the system was locally open, and perhaps even involved more than one fluid at more than one temperature.

Finally, the unclassified leucogranite samples plot close to the South Mountain magmatic trend, and in contrast to their intrusive field relations, they appear chemically to be the associated type, i.e., products of hydrothermal alteration. Their relatively unevolved compositions suggest that either the alteration was slight, or the unaltered protolith was somewhat more primitive than the fine-grained leucomonzogranite rocks that host other associated leucogranitic rocks.

## $^{40}Ar/^{39}Ar$ geochronology

### *Sampling and methods*

High-purity (>99%) muscovite separates were prepared by conventional techniques for three associated leucogranite bodies and nine independent ones (see Fig. 1 for sample locations). The separates were irradiated in the McMaster University nuclear reactor with the hornblende standard, MMHb-1, as a flux monitor. An age of 519 Ma was assumed for the hornblende (Alexander *et al.*, 1978). The analytical procedures employed in the Dalhousie University laboratory have been described in detail elsewhere (Muecke *et al.*, 1988).

Conventional argon release plots of the muscovite data are shown in Fig. 7; isotope correlation plots did not provide any useful additional information, so they are not shown. Each of the spectra has an apparent age plateau [according to the definition by Fleck *et al.* (1977)] involving at least 80% of the total gas released. The plateau ages ranging between $369 \pm 2$ Ma and $375 \pm 4$ Ma exhibit no variations beyond those expected from the analytical uncertainties. These uncertainties, quoted at the $1\sigma$ level, cover the measurement of the parameter $J$, but not the possible error in the assumed age of the hornblende standard.

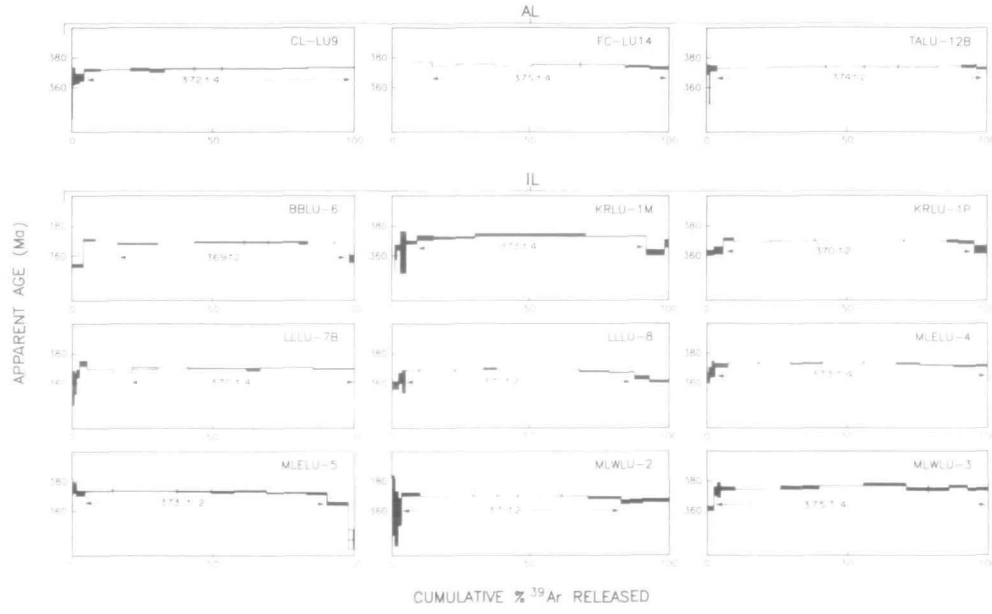


FIG. 7. $^{40}Ar/^{39}Ar$ age spectra for 12 muscovite separates from leucogranitic rocks; three from associated leucogranite (AL) samples across the top of the figure, and nine from independent leucogranite (IL) samples below. The double-ended arrow defines the extent of the plateau for each stated age. Vertical tick marks on the spectra indicate separate heating steps. Half-heights of black bars represent the relative (between-step) uncertainties at the $1\sigma$ level.

The mean plateau age of the present samples (calculated by weighting according to the inverse squares of the standard deviations) is $371{\cdot}5 \pm 2{\cdot}5$ Ma. This result is in remarkably good agreement with previous age determinations for the South Mountain Batholith as described above, and it supports the conclusion that, within analytical uncertainty, all isotopic systems in the batholith closed at about the same time.

*Results and interpretation of the geochronology*

Some of the South Mountain Rb–Sr and K–Ar isotopic systems have been disturbed. It should be recalled, however, that the Rb–Sr system in at least one muscovite from a leucomonzogranite appears to have resisted disturbance. Our $^{40}Ar/^{39}Ar$ data show no disturbances, except perhaps for the slight lowering of the apparent age of some samples over the first few percent of gas released. In an earlier reconnaissance study, Reynolds *et al.* (1981) reported a mean $^{40}Ar/^{39}Ar$ age of 367 Ma for mica from South Mountain Batholith rocks. It appears that the muscovite (both primary and secondary) in all the leucogranite samples has ages close to the intrusion age, and that no age $< 370$ Ma is primary. These represent slightly disturbed isotopic systems (Harper, 1988), but their cause is unknown. Possibly they result from the circulation of late-stage hydrothermal solutions, or tectono-thermal overprinting (Kontak & Cormier, 1991). The agreement at 372 Ma of three isotopic systems (U–Pb, Rb–Sr, and K–Ar), with different closure temperatures and different resistances to geochemical and thermal disturbance, raises an intriguing question about how a body the size of the South Mountain Batholith could intrude, crystallize, and cool so quickly.

## DISCUSSION

### *Origins of the leucogranitic rocks*

In the South Mountain Batholith, the following characteristics suggest that the independent leucogranite bodies are the products of the latest-stage, closed-system, fluid–magmatic processes: discrete plutons with sharp contacts; intimate spatial association with coarse-grained segregation pods and pegmatites; pervasive albitization; primary muscovite; highest levels of some incompatible elements (Li, Rb, U, F, Sn, W, and Pb); strongly fractionated HREE patterns; and a limited range of $\delta^{18}O$ values. The minerals and their textures appear to have formed by crystallization of water-saturated granitic melt at temperatures just above the solidus, and in part by reaction with the aqueous fluids that remained below the solidus.

The following characteristics of the associated leucogranites suggest that they formed as the products of post-magmatic, open-system, hydrothermal alteration of their fine-grained leucomonzogranitic host rocks: restricted sizes; gradational contacts; close spatial association with, and textures similar to, their host rocks; secondary muscovite; REE patterns similar to their host rocks; and highly variable $\delta^{18}O$ values. Thus, the minerals and textures of the associated leucogranites probably represent dominantly magmatic rocks hydrothermally altered to varying degrees at temperatures below the granite solidus.

On the basis of their field relations, the unclassified bodies appear to be of the independent type, but in most other geochemical respects, including $\delta^{18}O$ values but excluding $SiO_2$–A/CNK, they resemble either the associated type with a more primitive fine-grained leucomonzogranite precursor than the other associated bodies, or they may be truly independent leucogranites generated from a more primitive melt on the South Mountain magmatic trend (e.g., a parent silicate melt that reached $H_2O$-saturation at a much earlier stage in its chemical differentiation than the others).

*Relationships between leucogranitic rocks and mineral deposits*

The associated and independent leucogranite bodies both have spatially associated polymetallic mineral occurrences (Table 1), but the style of mineralization differs. Mineral occurrences in the independent bodies are either pegmatite-type (Sn, W, U, Mo, Li, Ta, and Cu) or dissemination- and/or fracture-type (U, F, Mo, and W). In contrast, three associated leucogranite bodies are affiliated with greisen and quartz vein-type occurrences (Cu, As, U, Sn, Mo, Pb, and Zn), and one associated leucogranite occurrence has disseminated U mineralization.

As noted above, several chemical parameters (e.g., K/Rb, F, and $P_2O_5$), indicate that the independent leucogranite bodies are the most evolved rocks in the eastern part of the South Mountain Batholith. The occurrence of mineralized and unmineralized pegmatite in many of these bodies suggests that most of them generated a fluid phase through 'second boiling'. The $\delta^{18}O$ values for the independent leucogranite rocks (+10·18 to +12·70‰; Table 2) indicate that the fluid–magmatic system was effectively closed, at least to external inputs (although the fluid itself may have escaped). The mineral occurrences in the independent leucogranites of this study, therefore, may represent localized concentrations of incompatible components from a volatile-rich fluid phase.

Our geochemical and age data support the formation of associated leucogranites by fluid–rock alteration at ~370 Ma, and A. K. Chatterjee (pers. comm., 1993) has estimated from whole-rock Pb–Pb data that the age of the Long Lake deposit, in an associated leucogranite body in the south central part of the batholith, is ~370 Ma. Thus, the associated leucogranites and their mineralization may have formed from related fluids. Our $\delta^{18}O$ data (+7·71 to +15·04‰; Table 2) suggest three possible origins for these fluids: (1) predominantly or entirely evolved from the granitic magmas with $\delta^{18}O = 10$–11‰; (2) a mixture of granitic and metamorphic sources yielding high $\delta^{18}O$ values; and (3) a mixture of granitic and meteoric sources yielding low $\delta^{18}O$ values. Therefore, in contrast to the occurrences of independent leucogranites, some of the mineral occurrences in the associated leucogranites probably formed from the open-system circulation of fluids.

A question of some interest is whether the differences between the associated and independent leucogranite bodies are significant in terms of the relative mineral potential of the two types. The independent leucogranitic bodies satisfy most, if not all of the mineralogical and geochemical criteria set out for 'specialized' granites by Tischendorf (1977), so they hold potential for the discovery of new mineral deposits. The associated leucogranitic rocks also satisfy most of these criteria, although they show lower concentrations of 'granophile' elements (Sn, W, and U) than the independent ones. In fact, the fluids responsible for the formation of the associated leucogranite bodies may have originated from underlying bodies of independent leucogranite. Thus, economically significant deposits could have formed near both types of leucogranite.

## CONCLUSIONS

(1) Two types of leucogranitic rocks occur in the South Mountain Batholith. They differ in their field relations (sharpness of contact and association with host rock), in mineralogy (particularly the amount of micas, the presence or absence of topaz, and the composition of plagioclase), and in chemical composition (especially $P_2O_5$, F, Rb, Nb, Ta, Gd/Yb, and, in some cases, $\delta^{18}O$) values.

(2) The associated leucogranite bodies appear to be the products of open-system hydrothermal alteration of the fine-grained leucomonzogranitic rocks because of their

restricted size, gradational contacts with fine-grained leucomonzogranite, similarity of their REE patterns to their host rocks, and highly variable $\delta^{18}O$ values.

(3) The independent leucogranite bodies appear to be the products of closed-system, late-stage crystallization in a fluid–magmatic regime on the basis of their occurrence as discrete bodies, pervasive albitization, high levels of incompatible elements, very low K/Rb ratios, strongly fractionated HREE patterns, and restricted $\delta^{18}O$ values.

(4) The unclassified leucogranite bodies at Walsh Brook are similar to the independent type of leucogranite in their field relations, but in most geochemical respects, including $\delta^{18}O$ values but excluding $SiO_2$–A/CNK variations, they are more like the associated leucogranite bodies, but with a protolith more primitive than the fine-grained leucomonzogranite precursors of any other.

(5) Field, mineralogical, and geochemical distinctions between the two leucogranitic types are matched by some differences in the styles of mineralization. The associated leucogranite bodies tend to be of the open-system greisen type, whereas the independent bodies tend to be of the closed-system pegmatite style of mineralization. There are also differences in the dominant metal associations of the two types.

(6) Our $^{40}Ar/^{39}Ar$ muscovite ages agree, within the limits of analytical precision, with Rb–Sr muscovite ages and U–Pb monazite determinations, suggesting that all these isotopic systems closed at $\sim$370 Ma, perhaps reflecting the rapid uplift indicated by the field relations.

## ACKNOWLEDGEMENTS

D.B.C., P.H.R., and F.J.L. acknowledge generous support from the Natural Sciences and Engineering Research Council (NSERC). Peter Elias provided field assistance and sample preparation in the early stages. Linda Richard and Bob MacKay analyzed the plagioclases by electron microprobe. Nelson Eby of the University of Massachusetts at Lowell kindly analyzed 16 of the samples by neutron activation. Joe Campbell and co-workers at NSDNR prepared the final figures.

## REFERENCES

Alexander, E. C., Michelson, G. M., & Lanphere, M. A., 1978. MMHb-1: a new $^{40}Ar/^{39}Ar$ dating standard. *Short Paper, 4th Int. Conf. Geochronology, Cosmology and Isotopic Geology. U.S. Geol. Surv. Open-File Rep.* **78-701**, 6–8.

Charest, M. H., 1976. Petrology, geochemistry and mineralization of the New Ross area, Lunenburg County, Nova Scotia. Unpublished M.Sc. Thesis, Dalhousie University, 154 pp.

Chatterjee, A. K., 1992. Radiometric lead as a chemical variable in peraluminous granites and greisens, South Mountain Batholith, Meguma Zone, Nova Scotia. *Geol. Assoc. Canada and Miner. Assoc. Canada, Joint Annual Meeting (Wolfville, Nova Scotia), Prog. Abstr.* **17**, A16.

—— Clarke, D. B., 1985. Guide to the granites and mineral deposits of South-western Nova Scotia. *Nova Scotia Dep. Mines Energy Open File Rep.* **650**, 264 pp.

—— Muecke, G. K., 1982. Geochemistry and the distribution of uranium and thorium in the granitic rocks of the South Mountain Batholith, Nova Scotia: some genetic and exploration implications. In: Maurice, Y. T. (ed.) *Uranium in Granites. Geol. Surv. Canada Paper* **81-23**, 11–17.

—— Strong, D. F., 1985. Geochemical characteristics of the polymetallic tin domain, southwestern Nova Scotia, Canada. In: Taylor, R. P., & Strong, D. F. (eds.) *Granite-Related Mineral Deposits: Geology, Petrogenesis, Tectonic Setting. CIM Conference, Halifax, Extended Abstracts*, Montreal, Quebec: Canadian Institute of Mining, 41–52.

—— —— Clarke, D. B., Robertson, J., Pollock, D., & Muecke, G. K., 1985. Geochemistry of the granodiorite hosting uranium mineralization at Millet Brook. In: Chatterjee, A. K., & Clarke, D. B. (eds.) *Guide to the Granites and Mineral Deposits of Southwestern Nova Scotia. Nova Scotia Dep. Mines Energy Paper* **85-3**, 63–114.

Clarke, D. B., & Chatterjee, A. K., 1988. Physical and chemical processes in the South Mountain batholith. In:

Taylor, R. P., & Strong, D. F. (eds.) *Granite-Related Mineral Deposits*. Montreal, Quebec: Canadian Institute of Mining and Metallurgy, Spec. Vol. **39**, 223–33.

—— Halliday, A. N., 1980. Strontium isotope geology of the South Mountain Batholith, Nova Scotia. *Geochim. Cosmochim. Acta* **44**, 1045–58.

—— —— Hamilton, P. J., 1988. Neodymium and strontium isotopic constraints on the origin of the peraluminous granitoids of the South Mountain batholith, Nova Scotia, Canada. *Chem. Geol.* **73**, 15–24.

—— Muecke, G. K., 1985. Review of the petrochemistry and origin of the South Mountain Batholith and associated plutons, Nova Scotia, Canada. In: *High Heat Production (HHP) Granites, Hydrothermal Circulation and Ore Genesis*. London: Inst. Min. Metall., 41–54.

Clayton, R. N., & Mayeda, T. K., 1963. The use of bromine pentafluoride in the extraction of oxygen from oxides and silicates for isotopic analysis. *Geochim. Cosmochim. Acta* **27**, 43–52.

Corey, M. C., 1987. Bedrock geological map of Mount Uniacke, NTS sheet 11D/13 (west half). Nova Scotia Department of Mines and Energy, Map **87-8**, scale 1:50 000.

—— 1991. Geological map of Chester, NTS sheet 21A/09. Nova Scotia Department of Mines and Energy, Map **90-9**, scale 1:50 000.

Craig, H., 1961. Standards for reporting concentrations of deuterium and oxygen-18 in natural waters. *Science* **133**, 1833–4.

Eberz, G. W., Clarke, D. B., Chatterjee, A. K., & Giles, P. S., 1991. The chemical and isotopic composition of the lower crust beneath the Meguma Zone, Nova Scotia: evidence from granulite facies xenoliths. *Contr. Miner. Petrol.* **109**, 69–88.

Evans, A. M., 1982. *Metallization Associated with Acid Magmatism*. New York: John Wiley, 385 pp.

Farley, E. J., 1978. Mineralisation at the Turner and Walker Deposits, South Mountain Batholith. Unpublished M.Sc. Thesis, Dalhousie University, 252 pp.

Fleck, R. J., Sutter, J. F., & Elliott, D. H., 1977. Interpretation of discordant $^{40}Ar/^{39}Ar$ age-spectra of Mesozoic tholeiites from Antarctica. *Geochim. Cosmochim. Acta* **41**, 15–32.

Groves, D. I., & McCarthy, T. S., 1978. Fractional crystallization and the origin of tin deposits in granitoids. *Miner. Deposita* **13**, 11–26.

Ham, L. J., 1991. Geological map of Windsor, NTS sheets 21A/16 (west half) and part of 21H/01. Nova Scotia Department of Mines and Energy, Map **90-10**, scale 1:50 000.

—— Marsh, S. W., Corey, M. C., Horne, R. J., & MacDonald, M. A., 1989. Lithogeochemistry of the eastern portion of the South Mountain Batholith, Nova Scotia. *Nova Scotia Dep. Mines Energy Open File Rep.* **89-001**, 62 pp.

Harper, C. L., 1988. On the nature of time in the cosmological perspective. Unpublished Ph.D. Thesis, Oxford University, 508 pp.

Horne, R. J., 1987. Preliminary geology map of New Germany NTS sheet 21A/10. Nova Scotia Department of Mines and Energy, Open File Map **87-004**, scale 1:50 000.

—— Corey, M. C., Ham, L. J., & MacDonald, M. A., 1988. Primary and secondary structural features in the eastern portion of the South Mountain Batholith, southwestern Nova Scotia: implications for regional stress orientations during intrusion. *Maritime Sediments Atlantic Geol.* **24**, 71–82.

Keppie, J. D., & Dallmeyer, R. D., 1987. Dating transcurrent terrane accretion: an example from the Meguma and Avalon composite terranes in the northern Appalachians. *Tectonics* **6**, 831–47.

Kontak, D. J., 1990. The East Kemptville topaz-muscovite leucogranite, Nova Scotia I. Geological setting and whole-rock geochemistry. *Can. Miner.* **28**, 787–825.

—— Cormier, R. F., 1991. Geochronological evidence for multiple tectono-thermal overprinting events in the East Kemptville muscovite–topaz leucogranite, Yarmouth County, Nova Scotia, Canada. *Can. J. Earth Sci.* **28**, 209–44.

—— Strong, D. F., & Kerrich, R., 1988. Crystal–melt ± fluid phase equilibria versus late-stage fluid–rock interaction in granitic rocks of the South Mountain Batholith, Nova Scotia: whole rock geochemistry and oxygen isotope evidence *Maritime Sediments Atlantic Geol.* **24**, 97–110.

Kovalenko, V. I., Antipin, V. S., Konusova, V. V., Smirnova, Y. V., Petrov, L. L., Vladykin, N. V., Kuznetsova, A. I., Kostyukova, Y. S., & Pisarskaya, V. A., 1977. Partition coefficients of fluorine, niobium, tantalum, lanthanum, ytterbium, yttrium, tin and tungsten in ongonite. *Dokl. Akad. Nauk SSSR (Earth Sci. Section)* **233**, 203–5.

Logothetis, J., 1984. The mineralogy and geochemistry of metasomatized rocks from occurrences in the South Mountain Batholith: New Ross Area, southwestern Nova Scotia. Unpublished M.Sc. Thesis, Dalhousie University, 359 pp.

London, D., Hervig, R. L., & Morgan, G. B., 1988. Melt–vapor solubilities and element partitioning in peraluminous granite–pegmatite systems: experimental results with Macusani glass at 200 MPa. *Contr. Miner. Petrol.* **99**, 360–73.

Longstaffe, F. J., Smith, T. E., & Muelenbachs, K., 1980. Oxygen isotope evidence for the genesis of Upper Paleozoic granitoids from southwestern Nova Scotia. *Can. J. Earth Sci.* **17**, 132–41.

MacDonald, M. A., & Clarke, D. B., 1991. Use of nonparametric ranking statistics to identify magmatic and post-magmatic processes in the eastern South Mountain Batholith, Nova Scotia, Canada. *Chem. Geol.* **92**, 1–20.

—— Ham, L. J., 1992. Geological map of Gaspereau Lake, NTS sheets 21A/15 and part of 21H/02. Nova Scotia Department of Mines and Energy, Map **92-1**, scale 1:50 000.
—— Horne, R. J., 1987. Bedrock geological map of Halifax and Sambro NTS sheets 11D/12 and part of 11D/05. Nova Scotia Department of Mines and Energy, Map **87-6**, scale 1:50 000.
—— —— Corey, M. C., & Ham, L. J., 1992. An overview of recent bed-rock mapping and follow-up petrological studies of the South Mountain Batholith, southwestern Nova Scotia, Canada. *Atlantic Geol.* **28**, 7–28.
McKenzie, C. B., 1974. Petrology of the South Mountain Batholith, Western Nova Scotia. Unpublished M.Sc. Thesis, Dalhousie University, 101 pp.
—— Clarke, D. B., 1975. Petrology of the South Mountain batholith, Nova Scotia. *Can. J. Earth Sci.* **12**, 1209–18.
Monier, G., Mergoil-Daniel, J., & Labernardière, H., 1984. Générations successives de muscovites et feldspaths potassiques dans les leucogranites du massif de Millevaches (Massif Central français). *Bull. Minér.* **107**, 55–68.
Montel, J. M., Mouchel, R., & Pichavant, M., 1988. High apatite solubilities in peraluminous melts. *Terra Cognita* **8**, 71.
Muecke, G. K., & Clarke, D. B., 1981. Geochemical evolution of the South Mountain batholith, Nova Scotia: rare-earth-element evidence. *Can. Miner.* **19**, 133–45.
—— Elias, P., & Reynolds, P. H., 1988. Hercynian/Alleghanian overprinting of an Acadian Terrane: $^{40}Ar/^{39}Ar$ studies in the Meguma Zone, Nova Scotia, Canada. *Chem. Geol.* **73**, 153–67.
O'Neil, J. R., & Taylor, H. P., Jr., 1967. The oxygen isotope and cation exchange chemistry of feldspars. *Am. Miner.* **52**, 1414–37.
O'Reilly, G. A., Farley, E. J., & Charest, M. H., 1982. Metasomatic–hydrothermal mineral deposits of the New Ross–Mahone Bay area, Nova Scotia. *Nova Scotia Dep. Mines Energy Paper* **82-2**, 96 pp.
—— Gauthier, G., & Brooks, C., 1985. Three Permo-Carboniferous Rb/Sr age determinations from the South Mountain Batholith, southwestern Nova Scotia. In: Mills, K. A., & Bates, J. L. (eds.) *Mines & Minerals Branch, Report of Activities 1984. Nova Scotia Dep. Mines Energy Rep.* **85-1**, 143–52.
Öhlander, B., Billström, K., & Hålenius, E., 1989. Behaviour of rare-earth elements in highly evolved granitic systems: evidence from Proterozoic molybdenite mineralized aplites and associated granites in northern Sweden. *Lithos* **23**, 267–80.
Parker, R. L., & Fleisher, M., 1968. Geochemistry of niobium and tantalum. *U.S. Geol. Surv. Prof. Paper* **612**, 43 pp.
Ponader, C. W., & Brown, G. E., 1989. Rare earth elements in silicate glass/melt systems: II. Interactions of La, Gd, and Yb with halogens. *Geochim. Cosmochim. Acta* **53**, 2905–14.
Reynolds, P. H., Zentilli, M., & Muecke, G. K., 1981. K–Ar and $^{40}Ar/^{39}Ar$ geochronology of granitic rocks from southern Nova Scotia: its bearing on the geological evolution of the Meguma Zone of the Appalachians. *Can. J. Earth Sci.* **18**, 386–94.
Richardson, J. M., Bell, K., Blenkinsop, J., & Watkinson, D. H., 1989. Rb–Sr age and geochemical distinctions between the Carboniferous tin-bearing Davis Lake complex and the Devonian South Mountain Batholith, Meguma Terrane, Nova Scotia. *Ibid.* **26**, 2044–61.
Searle, M. P., & Fryer, B. J., 1986. Garnet, tourmaline and muscovite-bearing leucogranites, gneisses and migmatites of the Higher Himalayas from Zanskar, Kulu, Lahoul and Kashmir. In: Coward, M. P., & Ries, A. C. (eds.) *Collision Tectonics. Geol. Soc. Spec. Publ.* **19**, 185–201.
Shaw, D. M., 1968. A review of K–Rb fractionation trends by covariance analysis. *Geochim. Cosmochim. Acta* **32**, 573–601.
Smith, T. E., 1974. The geochemistry of the granitic rocks of Halifax County, Nova Scotia. *Can. J. Earth Sci.* **11**, 650–8.
—— Peck, D., Huang, C. H., & Holm, P. E., 1986. A re-appraisal of the alaskite/muscovite–biotite granite suite of Halifax County, Nova Scotia. *Maritime Sediments Atlantic Geol.* **22**, 101–16.
Smitheringale, W. G., 1973. Geology of parts of Digby, Bridgtown, and Gaspereau Lake map-areas, Nova Scotia. *Geol. Surv. Canada Mem.* **379**, 74 pp.
Streckeisen, A., 1976. To each plutonic rock its proper name. *Earth-Sci. Rev.* **12**, 1–33.
Strong, D. F., 1988. A review and model for granite-related mineral deposits. In: Taylor, R. P., & Strong, D. F. (eds.) *Recent Advances in the Geology of Granite-Related Mineral Deposits.* Montreal, Quebec: Canadian Institute of Mining and Metallurgy, Spec. Vol. **39**, 424–45.
—— Hanmer, S. K., 1981. The leucogranites of southern Brittany: origin by faulting, frictional heating, fluid flux and fractional melting. *Can. Miner.* **19**, 163–76.
Taylor, F. C., 1969. Geology of the Annapolis–St. Mary's Bay map-area, Nova Scotia. *Geol. Surv. Canada Mem.* **358**, 65 pp.
Taylor, H. P., Jr., 1968. The oxygen isotope geochemistry of igneous rocks. *Contr. Miner. Petrol.* **19**, 1–71.
—— 1978. Oxygen and hydrogen isotope studies of plutonic granitic rocks. *Earth Planet. Sci. Lett.* **38**, 177–210.
Taylor, S. R., 1965. The application of trace element data to problems in petrology. *Phys. Chem. Earth* **6**, 133–213.
Tischendorf, G., 1977. Geochemical and petrographic characteristics of silicic magmatic rocks associated with rare-element mineralization. In: Stemprok, M., Burnol, L., & Tischendorf, G. (eds.) *Metallization Associated with Acid Magmatism*, Vol. 2. Prague: Czech. Geol. Survey, 41–92.
Wang, Y.-R., Li, J.-T., Lu, J.-T., & Fan, W.-L., 1982. Geochemical mechanism during the late stage of granite crystallization. *Geochemistry (Beijing)* **1**, 175–85.